*Pak. J. Bot.*, 58(10): October, 2026.

**ARTICLE** **DOI: http://dx.doi.org/10.30848/PJB2026-10(2)**

# GENOME-WIDE IDENTIFICATION OF THE BRASSINOSTEROID-SIGNALING KINASE (BSK) GENE FAMILY IN *BRASSICA NAPUS*

**KEMING ZHU[1†], WENDA ZHAO[1†], REHMAN SARWAR[1], QINGFENG MENG[1], HONGFEI GUO[1], ZHICHUANG JIN[1] AND XIAOLI TAN[1*]**

[1]School of Life Sciences, Jiangsu University, Zhenjiang 212013, China
[†]These authors contributed equally to this work
Postal: 212013, ORCID: 0000-0002-9358-605X, Tel.: +86-511-88785506; Fax: +86-511-88791923

*Corresponding author's email: xltan@ujs.edu.cn

**Abstract**

Brassinosteroid signaling kinases (BSKs) are a class of plant-specific receptor-like cytoplasmic kinases that are integral to brassinosteroid (BR) signal transduction. In *Brassica napus*, a total of 37 *BnaBSK* genes were identified and phylogenetically grouped into eight distinct groups. These genes were located on 17 chromosomes and 2 scaffolds, with 5 members clustered on the C09 chromosome. These proteins contain kinase domains and tetrapeptide repeats and predominantly exhibit acidic properties. The promoters of *BnaBSK* genes are enriched with stress-responsive *cis*-elements, particularly those induced by the hormone auxin and anoxia, suggesting a potential role in modulating plant development and metabolism. The expression patterns of *BnaBSK* genes vary under multiple stress conditions, and several members demonstrate high expression levels across all tissues of oilseed rape throughout its development phase, pointing to the *BnaBSK* genes contributing to the growth and adaptation. This study investigates the potential roles of BnaBSKs in the growth, development, and stress response of *B. napus*.

**Key words:** *Brassica napus*; *BSK* gene family; Development; Systematic evolution; Gene duplication

## Introduction

*Brassica napus* L., a globally esteemed oilseed crop, boasts a multifaceted significance, serving as a nutritious vegetable, a source of edible oil, and a vital component in animal feed production (Chalhoub *et al.*, 2014; Chen *et al.*, 2022). Its intricate growth and development processes are orchestrated by a complex interplay of plant hormones, among which brassinosteroids (BR) occupy a pivotal position. Brassinosteroids are a class of steroidal hormones widely distributed in plants (Clouse, 2011; Słomnicka *et al.*, 2025; Vukašinović *et al.*, 2025). First isolated from neem leaves in 1968, brassinosteroids were found to stimulate plant growth. Decades of research have since clarified their structure, diversity, and physiological roles. Currently acknowledged as the sixth major class of hormones found in plants, they exert profound effects on cellular activities, physiological responses, and developmental milestones within plants (Fàbregas & Caño-Delgado, 2014; Neu *et al.*, 2019). Furthermore, brassinosteroids interact with other hormones, such as auxin (IAA), gibberellin (GA), and cytokinin (CK), to regulate vegetative and reproductive processes (Bai *et al.*, 2012; Peres *et al.*, 2019; Xia *et al.*, 2021).

During the past two decades, extensive research on the model plant *Arabidopsis thaliana* has illuminated the BR signaling pathway. BRASSINOSTEROID INSENSITIVE1 (BRI1), the membrane-bound receptor kinase, serves as the primary sensor initiating downstream signaling for BR molecules (Wang *et al.*, 2001; Tang *et al.*, 2008). Upon binding to BR, a cascade of interactions occurs, where BRI1 KINASE INHIBITOR 1 (BKI1) dissociates from BRI1, enabling BRI1-ASSOCIATED KINASE1 (BAK1) to bind to BRI1 and form a heterodimer (Nolan *et al.*, 2020; Han *et al.*, 2023). This heterodimer phosphorylates and activates BR-SIGNALING KINASEs (BSKs) and the CONSTITUTIVE DIFFERENTIAL GROWTH1 (CDG1) kinase families. These, in turn, activate the PP1-type phosphatase BRI1-SUPPRESSOR1 (BSU1), which dephosphorylates and inactivates BRASSINOSTEROID INSENSITIVE2 (BIN2). Inactivation of BIN2 relieves its inhibition of the transcription factors BRASSINAZOLE-RESISTANT1 (BZR1) and BRI1-EMS-SUPPRESSOR1 (BES1), allowing them to regulate gene expression and amplify BR signaling (Fig. 1) (Kim *et al.*, 2009; Wang *et al.*, 2012). In particular, BSKs, as crucial downstream components, harbor a putative kinase catalytic (PKc) domain at the N-terminus and a C-terminal TPR domain, facilitating their interactions with various proteins (Shiu *et al.*, 2004). The BSKs belong to the receptor-like cytoplasmic kinase XII subfamily (RLCK-XII), and 12 members were found in *A. thaliana*, which is categorized within the cytoplasmic receptor kinase family (Zhang *et al.*, 2022; Zhao *et al.*, 2025).

Studies have shown that *bsk3-1* can reduce the sensitivity of plants to BR, while overexpression of *BSK1*, *BSK3*, and *BSK5* can restore the phenotype of *bri1-5* mutants, indicating that BSKs function downstream of BRI1. Furthermore, overexpression of *BSK1*, *BSK3*, and *BSK5* in the background of BR-deficient *det2-1* mutant can significantly inhibit the dwarf phenotype of the mutant, which is related to the selective expression of the target gene *DWF4* of BZR1, suggesting that BSKs can activate downstream BR signals (Tang *et al.*, 2008). BSK4, BSK6, BSK7, and BSK8 function in plant growth and BR (brassinosteroid) signal transduction,

Received: 04-11-2025 Revised: 26-02-2026 Accepted: 05-03-2026 Online: 13-05-2026

partially overlap with BSK3 in these biological processes (Sreeramulu *et al.*, 2013). In Arabidopsis, BSK3 regulates BR signaling during root structure formation under mild nitrogen deficiency (Jia *et al.*, 2019), functioning as a scaffold protein (Ren *et al.*, 2019). Furthermore, the *bsk5* loss-of-function mutant confers heightened sensitivity to both abscisic acid (ABA) treatment and salinity (Li *et al.*, 2012). Furthermore, BSK1, which functions as a receptor-like cytoplasmic kinase, is associated with plant immune responses (Gao *et al.*, 2024). The mutant *bsk1-1* can inhibit the tolerance of the *edr2* mutant to powdery mildew and ethylene-induced senescence phenotype (Shi *et al.*, 2022). *Arabidopsis* BSK1 is physiologically associated with the pathogen-associated molecular pattern receptor kinase FLAGELLIN SENSING2 (FLS2) (Yan *et al.*, 2018), which is involved in the forward regulation of PAMP-triggered immunity (PTI), inhibiting pathogen infection and proliferation, and boosting resistance to plant disease (Su *et al.*, 2021; Liu *et al.*, 2024). Silencing *OsBSK1-2* can inhibit the flagellin and chitin-induced immune response in rice (*Oryza sativa* L.) (Wang *et al.*, 2017; Wang *et al.*, 2024). These underscore BSKs as central regulatory nodes in modulating plant growth, development, and stress adaptation processes (Anwar *et al.*, 2018; Wu *et al.*, 2021; Khan *et al.*, 2023; Qanmber *et al.*, 2024; Zolkiewicz and Gruszka, 2024). The functional diversity and evolutionary role of the *BSK* gene family in *B. napus* are yet to be fully elucidated, despite substantial progress in understanding the BR signaling pathway and its components.

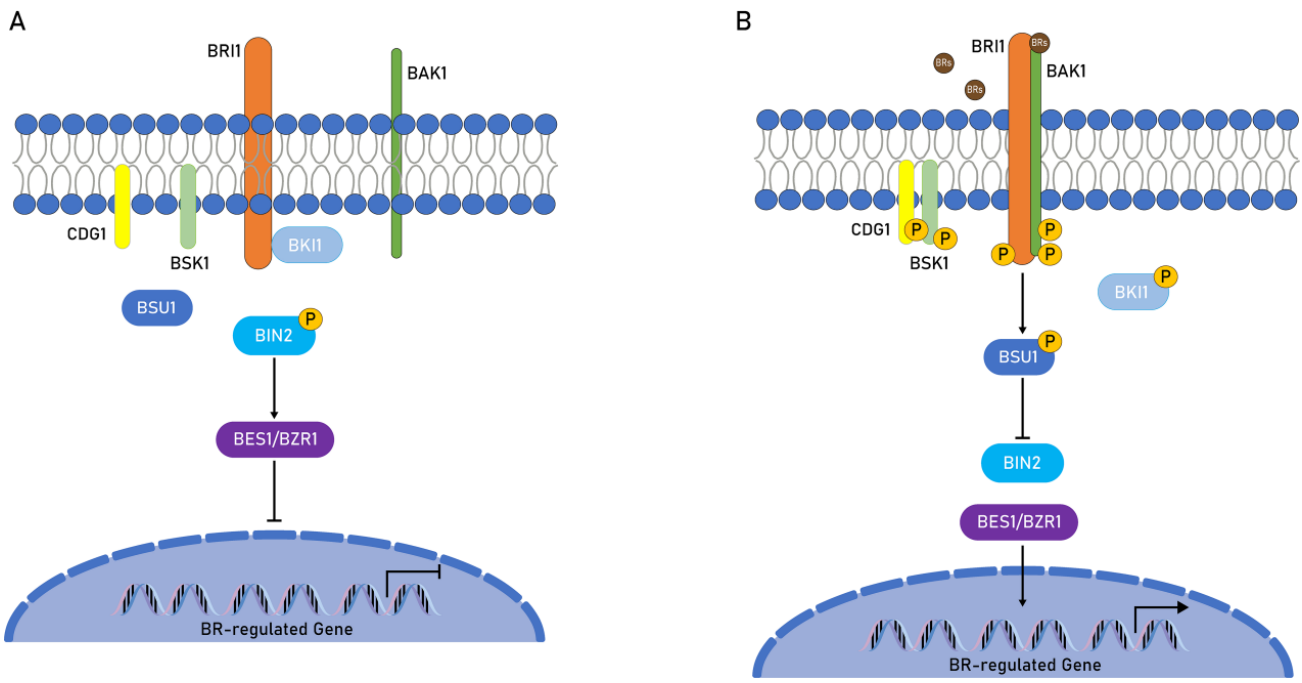


Fig. 1. Brassinosteroid signaling pathway. (A) In the absence of brassinosteroids (BR), BKI1 interacts with the receptor BRI1, rendering it inactive. Under these conditions, the kinase BIN2 remains active and phosphorylates the transcription factor BES1/BZR1. This phosphorylation prevents BES1/BZR1 from entering the nucleus, trapping it in the cytoplasm and thereby suppressing the expression of BR-responsive genes. (B) When brassinosteroid (BR) is present, it binds to the receptor BRI1 and its co-receptor BAK1, triggering transphosphorylation between them and causing BKI1 to dissociate from BRI1. Subsequently, the downstream signaling components BSK1 and CDG1 are phosphorylated by the activated BRI1-BAK1 receptor complex, which in turn activates the phosphatase BSU1, leading to the inactivation of BIN2. This results in the dephosphorylation of BES1/BZR1, causing them to accumulate in the nucleus and activate the expression of BR-responsive genes. The arrow indicates upregulate, while the horizontal line indicates downregulate and p indicates phosphorylation.

In this study, a total of 37 *BnaBSK* family members were identified genome-wide, followed by a systematic analysis of the phylogenetic relationships, subcellular localizations, protein motifs, gene structures, and *cis*-elements. The expression profiling of *BnaBSKs* in 8 different tissues (roots, stems, leaves, buds, shoot tips, flowers, mature siliques, and seeds) was also investigated. Additionally, transcriptome data offered preliminary predictions on BnaBSK expression patterns under various stress conditions, including drought, heat, cold, and phytohormone treatments (ABA, GA, IAA). Based on these findings, we further investigated the expression patterns of selected *BnaBSKs* using qRT-PCR following stress treatments, thus identifying potential candidates for functional validation. These observations suggest that BSKs are involved in coordinating growth processes, developmental programs, and stress signaling in *B. napus*.

## Materials and Methods

**Identification of gene family members:** Twelve *Arabidopsis* BSK protein sequences (AtBSKs) were obtained from the *Arabidopsis* genome database with corresponding Gene ID (*AT4G35230*, *AT5G46570*, *AT4G00710*, *AT1G01740*, *AT5G59010*, *AT3G54030*, *AT1G63500*, *AT5G41260*, *AT3G09240*, *AT5G01060*, *AT1G50990*, *AT2G17090*) (https://www.Arabidopsis.org/) (Lamesch *et al.*, 2012). And as queries, a BLAST P search was conducted using the *B. napus* Genome browser (BnPIR, http://cbi.hzau.edu.cn/bnapus), and the GENOSCOPE database (https://www.genoscope.cns.fr/brassicanapus/). Brassinosteroid signaling kinases (BSKs) in *B. rapa* and *B. oleracea* were retrieved through BLASTP analysis in the BRAD database (https://brassicadb.org/

brad/index.php). Additionally, genomic and coding sequences (CDSs) corresponding to homologs *in B. oleracea* and *B. rapa* were sourced directly from the BRAD platform (Cheng *et al.*, 2011). The candidate BSK proteins were verified using the NCBI (https://www.ncbi.nlm.nih.gov/cdd/), SMART (http://smart.embl-heidelberg.de/), and Pfam (http://xfam.org/) databases to remove redundancies, following established protocols (Letunic *et al.*, 2021; Mistry *et al.*, 2021). The molecular formula, isoelectric points, number of amino acids, and the molecular weight were calculated using the ExPASy proteomics server database (https://web.expasy.org/peptide_mass/), an online computational tool for protein analysis (Gasteiger *et al.*, 2003).

**Phylogenetic analyses of the BSK families in *B. napus*, *A. thaliana*, *B. rapa*, and *B. oleracea*:** Perform multiple sequence alignment using Muscle5 software with the deduced amino acid sequences of BSK proteins from *B. napus*, *Arabidopsis thaliana*, *B. rapa*, and *B. oleracea* (Edgar, 2022). TrimAl was used to trim the alignment results (parameter set to automated1). The optimal model (JTT+G4) was selected, and 5000 ultrafast bootstrap runs were completed. Maximum likelihood (ML) trees were generated using the IQ-TREE program (http://iqtree.cibiv.univie.ac.at/) (Minh *et al.*, 2020). To improve topological clarity and graphical presentation, tree visualization and annotation were performed using the iTOL online platform (https://itol.embl.de/) (Letunic & Bork, 2024).

**Analysis of the gene structure, conserved motifs, and conserved domain:** The Ensembl Plants database provided the *Arabidopsis thaliana* annotation files (Arabidopsis_thaliana.TAIR10.62: Ensembl Plants). The BnIR database provided the *B. napus* annotation files (Brassica_napus.ZS11.v0.gene: BnIR). TBtools software was used to evaluate and visualize the gene structures of members of the *BSK* gene family in *Brassica napus* and *Arabidopsis thaliana* based on their protein sequences and genome annotation data (Choi *et al.*, 2007; Chen *et al.*, 2023). With the default settings, conserved domains within the BSK proteins of *A. thaliana* and *B. napus* were mapped utilizing the Simple Modular Architecture Research Tool (SMART), Conserved Domain Database (CDD), and Pfam databases for consistency. Perform motif analysis on family member protein sequences using MEME Suite (https://meme-suite.org/meme/), with parameters set to identify 10 motifs.

**Chromosome location and collinearity analysis:** The *B. napus* genome database (BnPIR, http://cbi.hzau.edu.cn/bnapus) provided all of the *BnaBSKs* reference genomes (Brassica_napus.ZS11.v0.genome.fa) and their corresponding annotation files (Brassica_napus.ZS11.v0.gene.gff3). These were then mapped to their corresponding chromosomal locations using the TBtools software (Chen *et al.*, 2020). The MCScanX tool was used in TBtools for intra-species comparison analysis, and the gene collinearity was visualized by Advanced Circos. The syntenic analysis was conducted to identify orthologous *BSK* genes across *B. napus*, *A. thaliana*, *B. rapa*, and *B. oleracea*. Chromosomal localization and collinearity of genes were visualized through the Multiple Synteny Plot tool. To examine the selection patterns of each gene pair, compute the Ks values using TBtools. Using the formula T = Ks/2R, which calculates the divergence time (million years ago, Mya), the rate of divergence for nuclear genes, R, is $1.5 \times 10^{-8}$ synonymous substitutions per site per year for dicotyledonous plants (Koch *et al.*, 2000).

***Cis*-acting elements regulatory analysis:** The upstream promoter sequence spanning 2000 bp from the translation initiation site of the *BnaBSKs* was examined in the PlantCARE database (http://bioinformatics.psb.ugent.be/webtools/plantcare/html/) for *cis*-element analysis (Lescot *et al.*, 2002), and the *cis*-acting motifs positioning was then visualized by generating a map using TBtools (Chen *et al.*, 2020).

**Expression profiles analysis of *BnaBSKs*:** The *B. napus* transcriptome information resource (BnTIR) available at http://yanglab.hzau.edu.cn/BnTIR offered valuable insights into the *BSK* gene expression patterns throughout various developmental stages of *B. napus*. Additionally, this comprehensive database from Huazhong Agricultural University provided expression profiles of *BnaBSKs* under multiple stress conditions, specifically in leaf tissues (Liu *et al.*, 2021; Yang *et al.*, 2023). *BnaBSK* gene expression profiles were visualized by creating heat maps with the TBtools bioinformatics platform's HeatMap Illustrator module, normalized at the log2 scale (Chen *et al.*, 2020).

**Plant material, RNA extraction, and qRT-PCR:** *B. napus* seeds were germinated and grown at room temperature under the following conditions: 20 ± 5°C, a 16h light/8h dark photoperiod, a light intensity of 50 µmol/m²/s, and 70% relative humidity. Subsequently, the seedlings were transferred to Hoagland solution and cultivated until the four-leaf stage. To simulate salt and drought stress, the seedlings were treated with 1.2% NaCl and 10% PEG for 36 hours, respectively. Plant materials were then collected at 0, 3, 6, 12, 24, and 36 hours after the start of treatment, immediately frozen in liquid nitrogen, and stored at -80°C for RNA extraction. RNA extraction and cDNA synthesis were performed following the method described by the previous study (Sarwar *et al.*, 2021). All gene-specific primers used in this study were designed using BrassicaEDB (https://brassica.biodb.org/) and are listed in Table S5. The Actin gene (GenBank ID: XM_013858992) was used as the reference control gene. Quantitative real-time PCR (qRT-PCR) analysis was conducted using an Applied Biosystems QuantStudio 1 Real-Time PCR System (Applied Biosystems, Shanghai, China). The relative expression levels of *BnaBSKs* were measured using the $2^{-\Delta\Delta Ct}$ method. The expression level at 0 hours was set as the control, and a *t*-test was employed to analyze significant differences between time points. The results were visualized using GraphPad Prism 8.0 software (Swift, 1997).

## Results

**Identification and phylogenetic analysis of *BSKs* in *B. napus*:** The genomes of *B. napus*, *B. rapa*, and *B. oleracea* contained 37, 19, and 21 *BSK* genes, respectively, according to local BLASTN and BLASTP analyses using 12 known *AtBSKs* as references. Considerable variability was observed in the predicted lengths of amino acid residues across all 37 BnaBSK proteins, ranging from 358 to 819 aa, with corresponding molecular weights from 40386.99 to 92725.96 Da. All members are acidic with

theoretical pI values <7, ranging from 5.17 to 6.44. Among these, BnaA03G0444400ZS stood out as having the highest molecular weight but the lowest pI value, and its gene structure was the most complex (comprising 15 exons and 14 introns) (Table S1). Similarly, Table S2 gives the *BSK* genes summary for the genomes of *B. oleracea* and *B. rapa*. The proteins derived from these genetic sequences varied between 441 and 506 amino acids in length, tipping the scales at molecular weights anywhere from 49836.8 to 57037.8 Da, sharing a comparable physicochemical profile with their BnaBSK counterparts in *B. napus*. Comparing gene numbers across the three species clearly revealed that *B. napus*, as an allopolyploid, underwent gene family expansion during evolution. The number of members in this expanded gene family is roughly equivalent to the combined total of the two diploid ancestral species. This finding corresponds to the genetic changes in conservation and elimination following genome duplication.

To elucidate the phylogenetic relationships between BSK proteins in *A. thaliana*, *B. napus*, *B. oleracea*, and *B. rapa*, a maximum likelihood (ML) phylogenetic tree was constructed with the IQ-TREE program. This phylogenetic tree, based on optimal model (JTT+G4), grouped the 89 *BSK* genes-comprising 12 AtBSKs, 37 BnBSKs, 21 BoBSKs and 19 BrBSKs-into 8 distinct groups labeled 1 through 8 (Fig. 2). Specifically, group 1 encompassed the AtBSK7 and AtBSK8 subfamily, Group 2 contained AtBSK3 and AtBSK4 subfamilies, Group 3 included the AtBSK5 and AtBSK6 subfamily, Group 4 consisted of the AtBSK9 and AtBSK10 subfamilies, Group 5 contained the AtBSK2 branch, Group 6 included AtBSK11 and AtBSK12 subfamily, and the seventh group held the AtBSK1 subfamily. In *B. napus*, these groups were populated by varying numbers of BSK members: six members were assigned to Group 1, four to Group 2, six to Group 3, five to Group 4, six to Group 5, six to Group 6, two to Group 7, and two to Group 8. While Group 5 included AtBSK2 and six BnaBSKs, AtBSK2 exhibited greater similarity to BnaA06G0423600ZS and BnaC07 G0249700ZS than to the remaining four BnaBSKs, hinting at potentially similar functional roles. Each *AtBSK* gene in *Arabidopsis* corresponded to multiple homologs in the *B. napus* genome, except for AtBSK10, aligning with a single homologous gene. This anomaly might be due to their loss or differentiation during evolution. The findings underscored a substantial expansion of *BSK* homologous genes in *B. napus* relative to *A. thaliana*, further reinforcing the notion that *BSK* genes within the same subfamily exhibit distinct or overlapping functionalities.

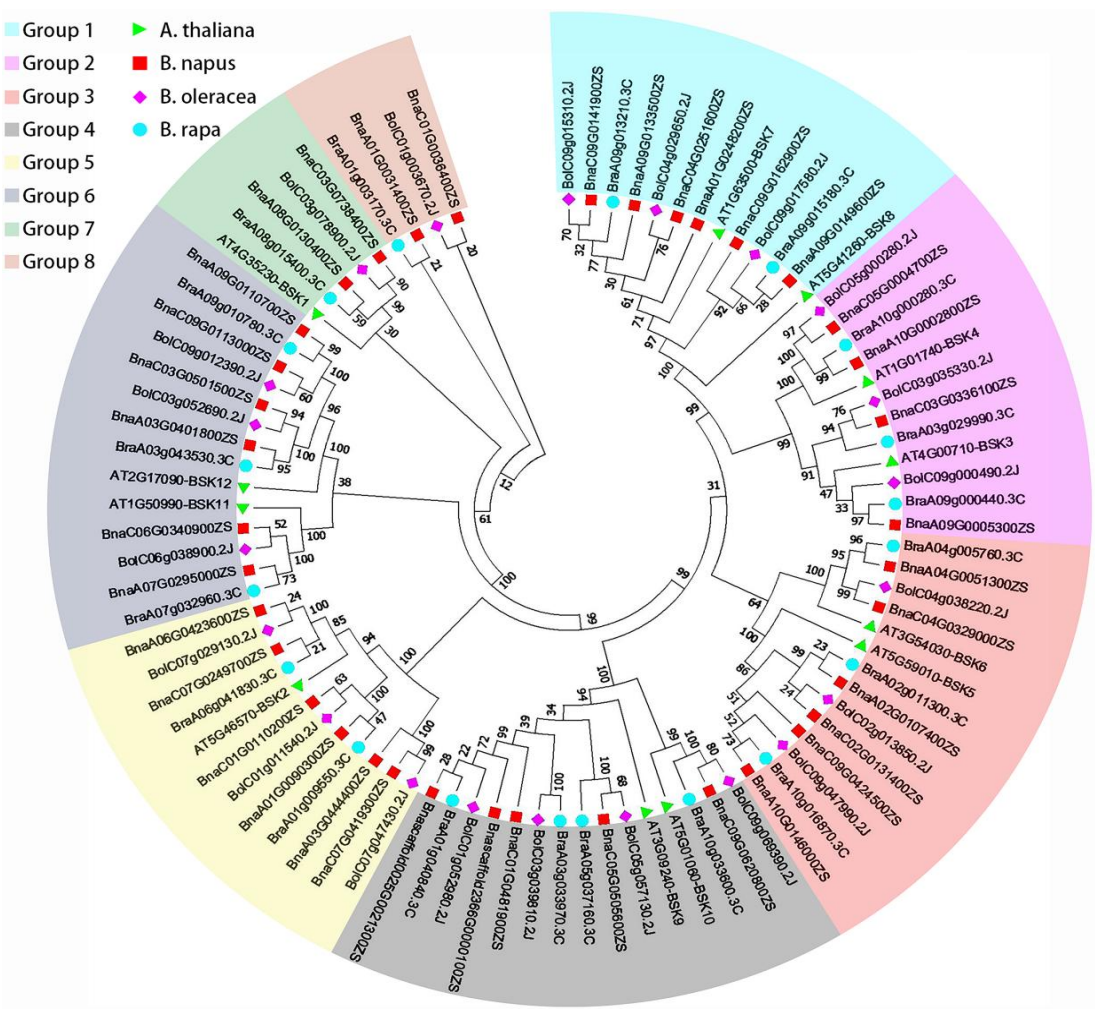


Fig. 2. The cladogram of BSKs proteins from *A. thaliana*, *B. napus*, *B. oleracea*, and *B. rapa*. Using the IQ-TREE program, a maximum likelihood (ML) phylogenetic tree was constructed based on BSK protein sequences from *Arabidopsis thaliana*, *B. napus*, *B. oleracea*, and *B. rapa*. Different colors in the figure represent the eight categories into which BSK proteins were clustered. The green triangle represents *A. Arabidopsis*, the red square represents *B. napus*, the pink diamond represents *B. oleracea*, and the blue circle represents *B. rapa*. The numbers on the nodes represent the self-expansion support rate (%) based on 5,000 repetitions.

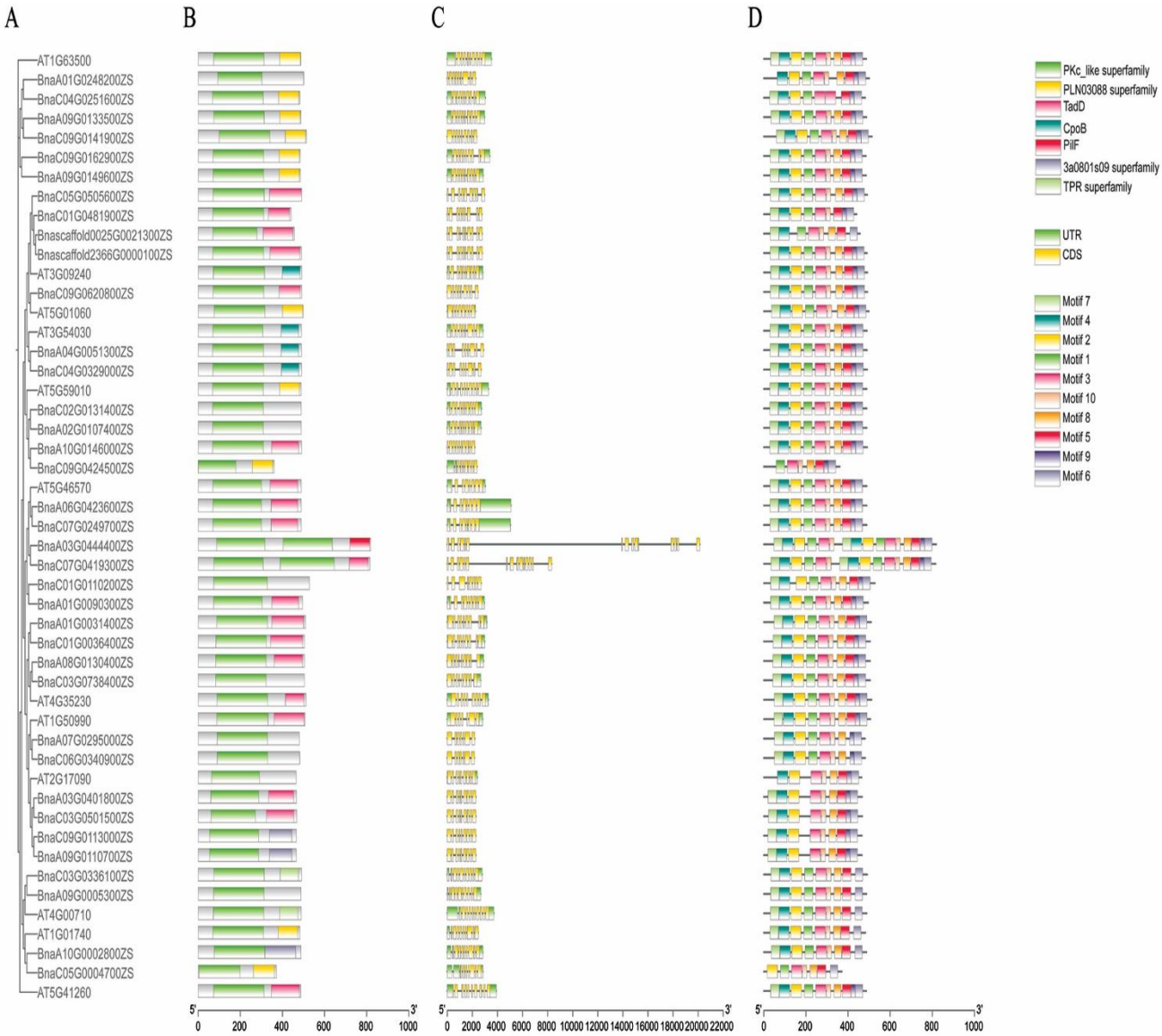


Fig. 3. Conserved motifs and gene structure analysis of the *BSK* gene family in *Brassica napus*. (A) Phylogenetic tree of the *Brassica napus BSK* gene Family. (B) Distribution of the conserved domains of the *BSK* gene in *Brassica napus*. (C) Structure of the *BSK* gene in *Brassica napus*, where yellow represents exons and green represents the 5' UTR and 3' UTR. (D) Schematic diagram of the distribution of conserved motifs in the *BSK* gene of *Brassica napus*, where different colors represent different conserved motifs.

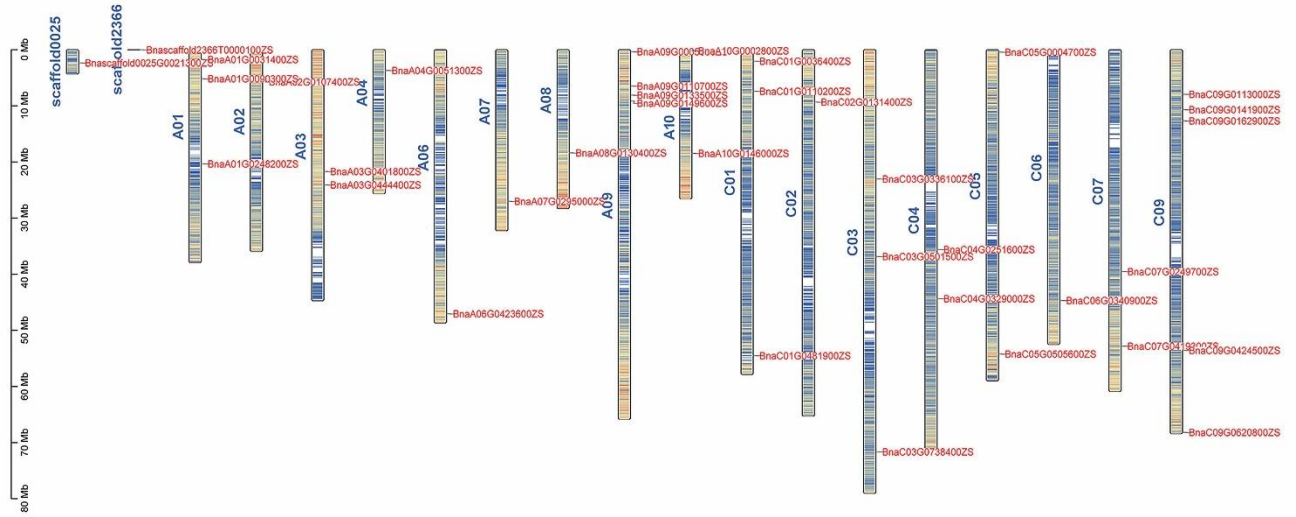


Fig. 4. Schematic representation of *BSK* genes distribution on *B. napus* chromosomes. The chromosomal number is annotated alongside each chromosome.

**Table S1. A complete list of 37 identified BnaBSKs in our study.**

| Gene name | gDNA size (bp) | CDS size (nts) | Peptide residues | Exon & Intron | Molecular weight | Theoretical pI | Molecular formula | At Orthologs | Location |
|---|---|---|---|---|---|---|---|---|---|
| BnaA01G0031400ZS | 3146 | 1533 | 510 | 9&8 | 56823.16 | 5.63 | $C_{2489}H_{3873}N_{699}O_{767}S_{30}$ | AT4G35230 | A01:1744821..1747967 |
| BnaA01G0090300ZS | 2951 | 1491 | 496 | 9&8 | 55824.68 | 5.35 | $C_{2469}H_{3887}N_{669}O_{751}S_{27}$ | AT5G46570 | A01:5166909..5169860 |
| BnaA01G0248200ZS | 2261 | 1506 | 501 | 9&8 | 55767.82 | 5.77 | $C_{2447}H_{3884}N_{676}O_{746}S_{33}$ | AT1G63500 | A01:20323637..20325898 |
| BnaA02G0107400ZS | 2692 | 1470 | 489 | 10&9 | 54672.1 | 5.52 | $C_{2424}H_{3782}N_{658}O_{735}S_{24}$ | AT5G59010 | A02:5717426..5720118 |
| BnaA03G0401800ZS | 2272 | 1404 | 467 | 9&8 | 52687.85 | 5.23 | $C_{2313}H_{3616}N_{628}O_{715}S_{32}$ | AT2G17090 | A03:21696716..21698988 |
| BnaA03G0444400ZS | 20132 | 2460 | 819 | 15&14 | 92725.96 | 5.17 | $C_{4118}H_{6411}N_{1107}O_{1261}S_{35}$ | AT5G46570 | A03:24068357..24088489 |
| BnaA04G0051300ZS | 2896 | 1473 | 490 | 9&8 | 55100.61 | 6 | $C_{2422}H_{3794}N_{678}O_{735}S_{29}$ | AT3G54030 | A04:3685158..3688054 |
| BnaA06G0423600ZS | 5080 | 1077 | 358 | 8&7 | 40588.52 | 5.59 | $C_{1811}H_{2842}N_{480}O_{540}S_{19}$ | AT5G46570 | A06:47040442..47045522 |
| BnaA07G0295000ZS | 2189 | 1446 | 481 | 7&6 | 54563.86 | 5.86 | $C_{2401}H_{3750}N_{670}O_{731}S_{27}$ | AT1G50990 | A07:27005947..27008136 |
| BnaA08G0130400ZS | 2943 | 1518 | 505 | 9&8 | 56470.92 | 5.58 | $C_{2475}H_{3873}N_{695}O_{761}S_{29}$ | AT4G35230 | A08:18377246..18380189 |
| BnaA09G0005300ZS | 2671 | 1467 | 488 | 10&9 | 55140.78 | 5.51 | $C_{2420}H_{3826}N_{670}O_{744}S_{29}$ | AT4G00710 | A09:342845..345516 |
| BnaA09G0110700ZS | 2269 | 1401 | 466 | 9&8 | 52762.97 | 6.4 | $C_{2327}H_{3645}N_{649}O_{703}S_{25}$ | AT2G17090 | A09:6469234..6471503 |
| BnaA09G0133500ZS | 2965 | 1467 | 488 | 10&9 | 54734.21 | 5.96 | $C_{2393}H_{3776}N_{678}O_{733}S_{30}$ | AT1G63500 | A09:8089276..8092241 |
| BnaA09G0149600ZS | 2868 | 1461 | 486 | 10&9 | 54302.65 | 6.05 | $C_{2369}H_{3735}N_{673}O_{729}S_{31}$ | AT1G63500 | A09:9159996..9162864 |
| BnaA10G0002800ZS | 2828 | 1467 | 488 | 10&9 | 55129.26 | 5.97 | $C_{2429}H_{3850}N_{670}O_{729}S_{32}$ | AT1G01740 | A10:183000..185828 |
| BnaA10G0146000ZS | 2197 | 1476 | 491 | 10&9 | 55008.33 | 5.71 | $C_{2433}H_{3790}N_{668}O_{740}S_{24}$ | AT5G59010 | A10:18460890..18463087 |
| BnaC01G0036400ZS | 2980 | 1083 | 360 | 9&8 | 40906.41 | 5.36 | $C_{1796}H_{2808}N_{494}O_{553}S_{23}$ | AT4G35230 | C01:2029394..2032374 |
| BnaC01G0110200ZS | 2706 | 1587 | 528 | 8&7 | 59474.07 | 5.63 | $C_{2641}H_{4146}N_{712}O_{790}S_{30}$ | AT5G46570 | C01:7393484..7396190 |
| BnaC01G0481900ZS | 2761 | 1326 | 441 | 9&8 | 50010.25 | 6.44 | $C_{2209}H_{3455}N_{613}O_{653}S_{30}$ | AT3G09240 | C01:54503711..54506472 |
| BnaC02G0131400ZS | 2727 | 1470 | 489 | 10&9 | 54672.1 | 5.52 | $C_{2424}H_{3782}N_{658}O_{735}S_{24}$ | AT5G59010 | C02:9311474..9314201 |
| BnaC03G0336100ZS | 2775 | 1476 | 491 | 10&9 | 55172.72 | 5.76 | $C_{2412}H_{3818}N_{674}O_{747}S_{30}$ | AT4G00710 | C03:23011583..23014358 |
| BnaC03G0501500ZS | 2278 | 1407 | 468 | 9&8 | 52904.17 | 5.25 | $C_{2336}H_{3648}N_{626}O_{717}S_{29}$ | AT2G17090 | C03:36838030..36840308 |
| BnaC03G0738400ZS | 2704 | 1518 | 505 | 9&8 | 56401.83 | 5.58 | $C_{2471}H_{3862}N_{692}O_{761}S_{30}$ | AT4G35230 | C03:71634416..71637120 |
| BnaC04G0251600ZS | 3028 | 1449 | 482 | 10&9 | 53958.33 | 5.95 | $C_{2360}H_{3727}N_{667}O_{724}S_{29}$ | AT1G63500 | C04:35583626..35586654 |
| BnaC04G0329000ZS | 2702 | 1476 | 491 | 9&8 | 55288.85 | 6.08 | $C_{2425}H_{3810}N_{682}O_{738}S_{30}$ | AT3G54030 | C04:44347633..44350335 |
| BnaC05G0004700ZS | 2834 | 1116 | 371 | 9&8 | 41927.38 | 5.91 | $C_{1851}H_{2933}N_{505}O_{548}S_{28}$ | AT1G01740 | C05:413783..416617 |
| BnaC05G0505600ZS | 2970 | 1476 | 491 | 9&8 | 55521.51 | 5.43 | $C_{2457}H_{3858}N_{662}O_{741}S_{31}$ | AT3G09240 | C05:54206722..54209692 |
| BnaC06G0340900ZS | 2163 | 1449 | 482 | 7&6 | 54731.99 | 5.61 | $C_{2415}H_{3758}N_{666}O_{736}S_{26}$ | AT1G50990 | C06:44664537..44666700 |
| BnaC07G0249700ZS | 5026 | 1470 | 489 | 8&7 | 54921.58 | 5.62 | $C_{2432}H_{3829}N_{661}O_{739}S_{24}$ | AT5G46570 | C07:39519071..39524097 |
| BnaC07G0419300ZS | 8318 | 2451 | 816 | 15&14 | 92394.87 | 5.24 | $C_{4114}H_{6418}N_{1100}O_{1251}S_{34}$ | AT5G46570 | C07:52796319..52804637 |
| BnaC09G0113000ZS | 2272 | 1401 | 466 | 9&8 | 52765.85 | 6.11 | $C_{2323}H_{3630}N_{648}O_{706}S_{26}$ | AT2G17090 | C09:7929420..7931692 |
| BnaC09G0141900ZS | 2346 | 1545 | 514 | 9&8 | 57805.82 | 5.96 | $C_{2552}H_{3988}N_{708}O_{766}S_{30}$ | AT1G63500 | C09:10675706..10678052 |
| BnaC09G0162900ZS | 3389 | 1458 | 485 | 10&9 | 54255.62 | 6.05 | $C_{2370}H_{3738}N_{672}O_{728}S_{30}$ | AT1G63500 | C09:12668850..12672239 |
| BnaC09G0424500ZS | 2372 | 1086 | 361 | 9&8 | 40386.99 | 5.67 | $C_{1791}H_{2803}N_{481}O_{544}S_{19}$ | AT5G59010 | C09:53561242..53563614 |
| BnaC09G0620800ZS | 2448 | 1479 | 492 | 9&8 | 55984.82 | 5.85 | $C_{2490}H_{3855}N_{675}O_{738}S_{29}$ | AT5G01060 | C09:68177421..68179869 |
| Bnascaffold0025G0021300ZS | 2778 | 1374 | 457 | 10&9 | 51694.23 | 6.41 | $C_{2283}H_{3581}N_{631}O_{677}S_{31}$ | AT3G09240 | scaffold0025:2334171..2336949 |
| Bnascaffold2366G0000100ZS | 2784 | 1473 | 490 | 10&9 | 55514.52 | 6.23 | $C_{2455}H_{3841}N_{677}O_{728}S_{32}$ | AT3G09240 | scaffold2366:3185..5969 |

**Table S2. A complete list of identified BraBSKs and BolBSKs in our study.**

| Gene name | gDNA size (bp) | CDS size (nts) | Peptide residues | Exon & Intron | Molecular weight | Theoretical pI | Molecular formula | At Orthologs | Location |
|---|---|---|---|---|---|---|---|---|---|
| BolC01g003670.2J | 3288 | 1518 | 505 | 9&8 | 56531.8 | 5.43 | $C_{2476}H_{3852}N_{692}O_{766}S_{30}$ | AT4G35230 | C01:2126172..2129459 |
| BolC01g011540.2J | 2687 | 1491 | 496 | 9&8 | 55854.7 | 5.3 | $C_{2469}H_{3889}N_{671}O_{751}S_{27}$ | AT5G46570 | C01:7057641..7060327 |
| BolC01g052980.2J | 2748 | 1473 | 490 | 10&9 | 55441.4 | 6.22 | $C_{2449}H_{3838}N_{676}O_{729}S_{32}$ | AT3G09240 | C01:49260162..49262909 |
| BolC02g013850.2J | 2271 | 1497 | 498 | 10&9 | 55512.1 | 5.6 | $C_{2461}H_{3843}N_{667}O_{746}S_{25}$ | AT5G59010 | C02:9706818..9709088 |
| BolC03g035330.2J | 2114 | 1371 | 456 | 9&8 | 51242.2 | 6.06 | $C_{2243}H_{3556}N_{628}O_{695}S_{25}$ | AT4G00710 | C03:23760882..23762995 |
| BolC03g039810.2J | 2589 | 1482 | 493 | 10&9 | 56164.9 | 8.42 | $C_{2506}H_{3948}N_{688}O_{718}S_{30}$ | AT3G09240 | C03:26376745..26379333 |
| BolC03g052690.2J | 2282 | 1326 | 441 | 10&9 | 49836.8 | 5.35 | $C_{2199}H_{3444}N_{594}O_{671}S_{28}$ | AT2G17090 | C03:37611683..37613964 |
| BolC03g078900.2J | 2369 | 1518 | 505 | 9&8 | 56401.8 | 5.58 | $C_{2471}H_{3862}N_{692}O_{761}S_{30}$ | AT4G35230 | C03:67520458..67522826 |
| BolC04g029650.2J | 2241 | 1449 | 482 | 10&9 | 53958.3 | 5.95 | $C_{2360}H_{3727}N_{667}O_{724}S_{29}$ | AT1G63500 | C04:30721448..30723688 |
| BolC04g038220.2J | 2711 | 1476 | 491 | 9&8 | 55338.9 | 6.08 | $C_{2429}H_{3812}N_{682}O_{738}S_{30}$ | AT3G54030 | C04:39415228..39417938 |
| BolC05g000280.2J | 2164 | 1467 | 488 | 9&8 | 55032 | 5.97 | $C_{2425}H_{3823}N_{673}O_{725}S_{32}$ | AT1G01740 | C05:154228..156391 |
| BolC05g057130.2J | 2816 | 1476 | 491 | 9&8 | 55519.5 | 5.43 | $C_{2458}H_{3860}N_{662}O_{742}S_{30}$ | AT3G09240 | C05:53094976..53097791 |
| BolC06g038900.2J | 2176 | 1431 | 476 | 7&6 | 54094.3 | 5.86 | $C_{2380}H_{3715}N_{665}O_{726}S_{26}$ | AT1G50990 | C06:39847861..39850036 |
| BolC07g029130.2J | 2346 | 1470 | 489 | 8&7 | 54921.6 | 5.62 | $C_{2432}H_{3829}N_{661}O_{739}S_{24}$ | AT5G46570 | C07:34637876..34640221 |
| BolC07g047430.2J | 3608 | 1509 | 502 | 9&8 | 57037.8 | 5.28 | $C_{2541}H_{3963}N_{677}O_{771}S_{22}$ | AT5G46570 | C07:47795558..47799165 |
| BolC09g000490.2J | 2218 | 1455 | 484 | 10&9 | 54551 | 5.73 | $C_{2388}H_{3775}N_{667}O_{737}S_{29}$ | AT4G00710 | C09:343056..345273 |
| BolC09g012390.2J | 2275 | 1401 | 466 | 9&8 | 52765.9 | 6.11 | $C_{2323}H_{3630}N_{648}O_{706}S_{26}$ | AT2G17090 | C09:8496971..8499245 |
| BolC09g015310.2J | 2347 | 1467 | 488 | 10&9 | 54699.2 | 6.05 | $C_{2394}H_{3779}N_{679}O_{731}S_{29}$ | AT1G63500 | C09:11398439..11400785 |
| BolC09g017580.2J | 2613 | 1458 | 485 | 10&9 | 54199.5 | 6.05 | $C_{2366}H_{3730}N_{672}O_{728}S_{30}$ | AT1G63500 | C09:13390352..13392964 |
| BolC09g047990.2J | 2220 | 1476 | 491 | 10&9 | 55035.2 | 5.49 | $C_{2430}H_{3783}N_{665}O_{747}S_{24}$ | AT5G59010 | C09:52543792..52546011 |
| BolC09g069390.2J | 2460 | 1479 | 492 | 9&8 | 55957.8 | 5.85 | $C_{2489}H_{3854}N_{674}O_{738}S_{29}$ | AT5G01060 | C09:67256840..67259299 |
| BraA01g003170.3C | 2737 | 1521 | 506 | 8&7 | 56209.7 | 5.61 | $C_{2483}H_{3862}N_{676}O_{758}S_{28}$ | AT4G35230 | A01:1559948..1562684 |
| BraA01g009550.3C | 2585 | 1491 | 496 | 9&8 | 55907.8 | 5.35 | $C_{2477}H_{3892}N_{670}O_{751}S_{26}$ | AT5G46570 | A01:4823634..4826218 |
| BraA01g040840.3C | 2859 | 1407 | 468 | 10&9 | 52808.4 | 6.08 | $C_{2327}H_{3660}N_{642}O_{699}S_{31}$ | AT3G09240 | A01:27467905..27470763 |
| BraA02g011300.3C | 2247 | 1488 | 495 | 10&9 | 55249.8 | 5.6 | $C_{2446}H_{3821}N_{665}O_{744}S_{25}$ | AT5G59010 | A02:5501668..5503914 |
| BraA03g029990.3C | 2168 | 1464 | 487 | 9&8 | 54730.3 | 5.86 | $C_{2395}H_{3792}N_{668}O_{739}S_{30}$ | AT4G00710 | A03:15094368..15096535 |
| BraA03g033970.3C | 3768 | 1413 | 470 | 10&9 | 53331.4 | 8.3 | $C_{2366}H_{3738}N_{646}O_{698}S_{29}$ | AT3G09240 | A03:16803615..16807382 |
| BraA03g043530.3C | 2281 | 1398 | 465 | 9&8 | 52416.5 | 5.17 | $C_{2302}H_{3595}N_{623}O_{714}S_{31}$ | AT2G17090 | A03:21975626..21977906 |
| BraA04g005760.3C | 2909 | 1473 | 490 | 9&8 | 55129.7 | 6.17 | $C_{2424}H_{3801}N_{679}O_{734}S_{29}$ | AT3G54030 | A04:3793707..3796615 |
| BraA05g037160.3C | 2841 | 1446 | 481 | 8&7 | 54726.7 | 5.73 | $C_{2423}H_{3812}N_{656}O_{727}S_{30}$ | AT3G09240 | A05:25696357..25699197 |
| BraA06g041830.3C | 2404 | 1470 | 489 | 8&7 | 54908.6 | 5.62 | $C_{2432}H_{3830}N_{660}O_{739}S_{24}$ | AT5G46570 | A06:27533375..27535778 |
| BraA07g032960.3C | 2188 | 1419 | 472 | 6&5 | 53598.9 | 6.11 | $C_{2379}H_{3702}N_{652}O_{714}S_{23}$ | AT1G50990 | A07:23690898..23693085 |
| BraA08g015400.3C | 2604 | 1398 | 465 | 8&7 | 51628.7 | 5.27 | $C_{2270}H_{3562}N_{624}O_{696}S_{28}$ | AT4G35230 | A08:12696241..12698844 |
| BraA09g000440.3C | 2177 | 1455 | 484 | 9&8 | 54659.2 | 5.66 | $C_{2396}H_{3787}N_{667}O_{737}S_{29}$ | AT4G00710 | A09:216673..218849 |
| BraA09g010780.3C | 2269 | 1401 | 466 | 9&8 | 52739.9 | 6.37 | $C_{2325}H_{3644}N_{648}O_{704}S_{25}$ | AT2G17090 | A09:6205184..6207452 |
| BraA09g013210.3C | 2322 | 1467 | 488 | 10&9 | 54676.1 | 5.96 | $C_{2390}H_{3770}N_{678}O_{732}S_{30}$ | AT1G63500 | A09:7775329..7777650 |
| BraA09g015180.3C | 2308 | 1518 | 485 | 10&9 | 54199.5 | 6.05 | $C_{2366}H_{3730}N_{672}O_{728}S_{30}$ | AT1G63500 | A09:8943877..8946184 |
| BraA10g000280.3C | 2132 | 1461 | 486 | 9&8 | 54929 | 5.97 | $C_{2420}H_{3834}N_{668}O_{726}S_{32}$ | AT1G01740 | A10:125369..127500 |
| BraA10g016870.3C | 2205 | 1437 | 478 | 10&9 | 53588.7 | 5.63 | $C_{2372}H_{3692}N_{650}O_{723}S_{22}$ | AT5G59010 | A10:12867829..12870033 |
| BraA10g033600.3C | 2374 | 1443 | 480 | 9&8 | 54354.8 | 5.35 | $C_{2412}H_{3743}N_{653}O_{727}S_{26}$ | AT5G01060 | A10:20614765..20617138 |

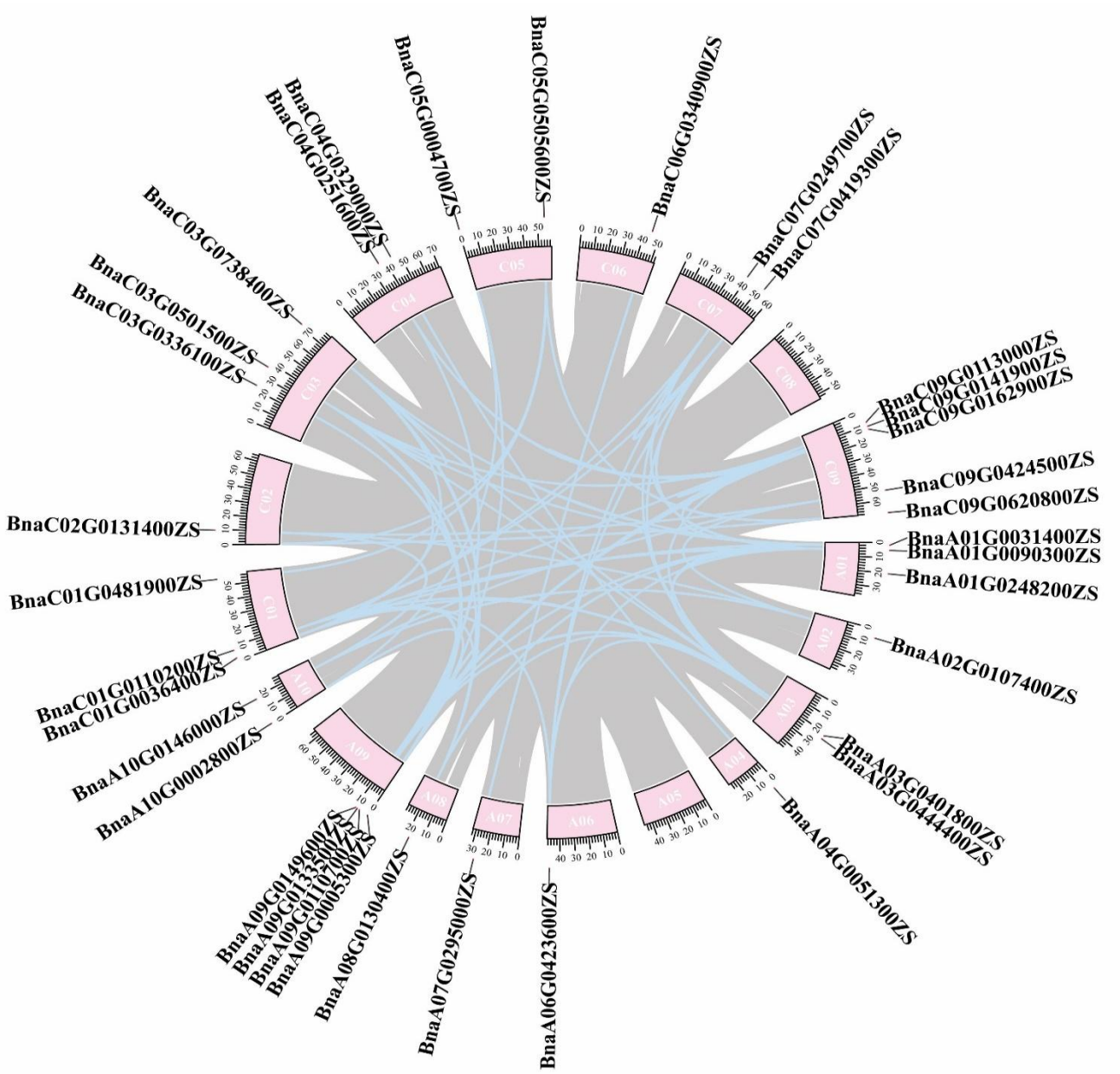


Fig. 5. Intraspecific collinearity analysis of the *BSK* gene family in *Brassica napus*. The chromosome is represented by the pink square, the collinear block in the *B. napus* genome is represented by the gray background, and the gene pairs with fragment repeats are connected by the blue line.

**Analysis of the *BnaBSK* gene structure, conserved domain, and conserved motif:** To construct a phylogenetic tree, 49 BSK protein sequences from rapeseed and *Arabidopsis* were arranged into separate clusters (Fig. 3A). The analysis delved into the domain architectures of the AtBSK and BnaBSK families. A salient feature of BSK proteins is the conserved N-terminal PKc (Putative kinase catalytic) domain, which is indispensable for their kinase activity, enabling them to phosphorylate targeted substrates. On the contrary, the C-terminal region exhibited flexibility, harboring 2 to 3 TPR domains that were crucial for mediating protein-protein interactions (Fig. 3B). PLN03088, TadD, CpoB, PilF, and the 3a0801s09 family all contain TPR domains. Analysis revealed that among the BnaBSK proteins, 9 lacked TPR domains, while others contained various domains: PLN03088 (11 proteins), TadD (19), CpoB (4), PilF (1), and 3a0801s09 (3). Only the AT4G00710 and BnaC03G0336100ZS proteins contained TPR structural domains. Remarkably, two *B. napus* members, BnaA03G0444400ZS and BnaC07G0419300ZS, possessed 2 kinase catalytic domains each-a feature unprecedented in the BSK family and not observed in *Arabidopsis*. This unique domain architecture suggested specialized roles in BR signaling or other physiological pathways. Truncations were observed at the N-terminus of two BSK proteins (BnaC05G0004700ZS and BnaC09G0424500ZS) in *B. napus*. This may lead to partial functional impairment or complete conversion into pseudogenes (Fig. 3B). In conclusion, the examination of the domain architectures of members of the BSK family not only enriched comprehension of this kinase family, but also provided potential clues, insights, and perspectives for advancing research on the BR signaling pathway, plant growth and development regulation, and crop genetic enhancement strategies.

Genomic organization contributes significantly to the gene family expansion and divergence (Wang *et al.*, 2015). An analysis of exon-intron structures within *BnaBSK* genes revealed diversity in exon number and length, exemplified

by the varying exons of 37 *BnaBSKs*, ranging from 7 to 15. The *BnaBSKs* within the same group shared similar structures, pointing to a close evolutionary linkage (Fig. 3C). Exon-intron structures exhibited consistency across different clusters; all 37 *BnaBSK* genes had both exons and introns and were less than 22 kb in length, 19 members lacked both 5'UTR and 3'UTR, while *BnaC07G0249700ZS* and *BnaA06G0423600ZS* contained extremely long UTRs. Beyond *BnaA03G0444400ZS* and *BnaC07G0419300ZS*, the number of exons in *BnaBSK* genes did not vary significantly, suggesting that they may share similar functions. In other words, structural variation may be associated with functional differentiation. This analysis underscored the intricate interplay between genomic organization and the evolutionary trajectories of gene families.

Conservative motif analysis revealed 10 characteristic motifs distributed across all 49 BSK family members. All BSKs contained motifs 2, 5, 6, and 10 (Fig. S1), which may represent key components contributing to functional specificity. BnaC09G0424500ZS and BnaC05G0004700ZS exhibited distinct motif deletion patterns, with their distribution positions differing from other family members. This variation may correlate with functional differentiation among gene family members (Fig. 3D). This gene family likely maintained its core functions through these conserved structures while achieving functional differentiation and evolution via diverse structural features. This enabled distinct gene members to play unique roles in the growth, development, and environmental adaptation of *B. napus*.

**Chromosome location and collinearity analysis:** Chromosomal localization analysis revealed that 37 *BnaBSK* genes were distributed on 17 chromosomes and two scaffolds (scaffold0025 and scaffold2366). Specifically, chromosomes A01, C01, and C03 each harbored 3 *BnaBSK* members; chromosomes A03, A10, C04, C05, and C07 each contained 2 *BnaBSK* members; chromosome A09 had 4 *BnaBSK* members, while chromosome C09 had 5 *BnaBSK* members. There was one *BnaBSK* member on the other seven chromosomes and two scaffolds, respectively (Fig. 4). These data show an uneven distribution of *BnaBSK* genes across the *B. napus* genome.

Collinearity analysis of *BnaBSK* genes on the 17 chromosomes revealed multiple pairs of repeated gene fragments. Within the rapeseed genome, we identified 68 duplicate gene pairs among 35 *BnaBSK* genes, all resulting from whole-genome duplication (WGD) or segmental duplication, with no tandem duplication events detected. The Ka/Ks ratios for all 68 gene pairs were less than 1 (ranging from 0.015 to 0.60), indicating strong purifying selection and functional conservation. Some gene pairs (BnaA06G0423600ZS/BnaC07G0249700ZS, Ka/Ks = 0.015) exhibited extremely low Ka/Ks ratios and recent divergence times, suggesting they may retain highly similar functions (Table S3). All these gene pairs were distributed across all 17 chromosomes and were almost equally distributed between the A and C subgenomes. Chromosome C09 exhibited the highest number of duplication events (5), while chromosomes A05 and C08 showed no distribution of duplication events (Fig. 5). Based on these observations, it was reasonable to infer that these paired genes arose through either whole-genome duplication or the duplication of extensive genetic fragments. This suggests that such large-scale duplication events represent a key driving force for the expansion and evolution of this gene family.

In order to explore the members of the phylogenetic functionality of the *BSK* gene family, the *BSK* gene families of *B. napus*, *A. thaliana*, *B. rapa*, and *B. oleracea* were collinearly analyzed. The analysis uncovered extensive *BSK* homologs shared among *B. napus* and the other 3 plants, with the highest number of homologs between *B. napus* and *B. oleracea* and the fewest homolog pairs with *A. thaliana*, indicating that *B. napus* exhibited more conserved synteny with different Brassicaceae plants within the *BSK* gene family (Ren *et al.*, 2021). There are one or more collinearity blocks between the *BnaBSKs* family members and *A. thaliana*, *B. rapa* and *B. oleracea*, suggesting that some homologous genes among the 4 species have undergone one more round of genome-wide replication, resulting in the dispersion or polymerization of some gene functions (Fig. 6). To examine the role of evolutionary forces and the nature of selective pressures, we computed the non-synonymous substitution rate (Ka), synonymous substitution rate (Ks), and their ratio (Ka/Ks) for homologous gene pairs in rapeseed and 3 crop species. Between rapeseed and *Arabidopsis*, *B. oleracea* and *B. rapa*, we found 43, 82, and 11 homologous *BSK* gene pairs, respectively (Ye *et al.*, 2023). The majority of homologous gene pairs (133/136), according to the results, had Ka/Ks ratios less than 1, suggesting that significant purifying selection was applied to these genes during evolution. Just a handful of gene pairs, like *BolC07g047430.2J.ml*/*BnaC07G0419300ZS* with a Ka/Ks ratio of 1.53, show a Ka/Ks value above 1, which points to these genes potentially having experienced positive selection or accelerated evolution after certain species split off. This pattern might tie into the development of functions unique to particular species and definitely calls for more in-depth study down the road (Table S4).

***Cis*-elements analysis of *BnaBSKs* gene promoters:** The promoter is a sequence on the DNA chain that can bind to RNA polymerase and initiate mRNA synthesis. It is an indispensable regulatory sequence for gene expression. Prediction of promoter sequences was carried out for the *B. napus BSKs* gene family, revealing *cis*-acting regulatory elements associated with various hormone pathways, as well as those linked to low temperature, stress, and developmental processes (Fig. 7). The distribution and abundance of these elements varied significantly among the *BnaBSK* promoters. Among them, *BnaC09T0424500ZS* had the highest number of functional components, suggesting it might act as a pleiotropic regulatory node involved in integrating multiple stress and developmental processes, whereas the promoters of *BnaA06T0192400ZS* and *BnaC07T0419300ZS* had the fewest. Among hormone-responsive elements, methyl jasmonate, auxin, and abscisic acid-related ones were markedly predominant, while those related to salicylic acid and gibberellin were less numerous. Enhancer-like elements specific to anoxic inducibility, anaerobic-related *cis*-acting elements, as well as elements responsive to low temperature and drought were also identified (Fig. 7), implying their possible functions in ecological stress responses. Only the promoters of *BnaA03T0401800ZS* and *BnaC09T0162900ZS* had *cis*-acting elements involved in cell cycle regulation (Fig. 7). Seed-specific regulatory elements detected exclusively on the promoters of *BnaA09T0013600ZS* and *Bna C09T0113000ZS* might participate in seed-related biological processes (Fig. 7). The diversity of *cis*-acting elements suggests that the *BnaBSK* gene may exhibit differential regulatory mechanisms in response to various biotic, abiotic, and hormonal stressors in plants.

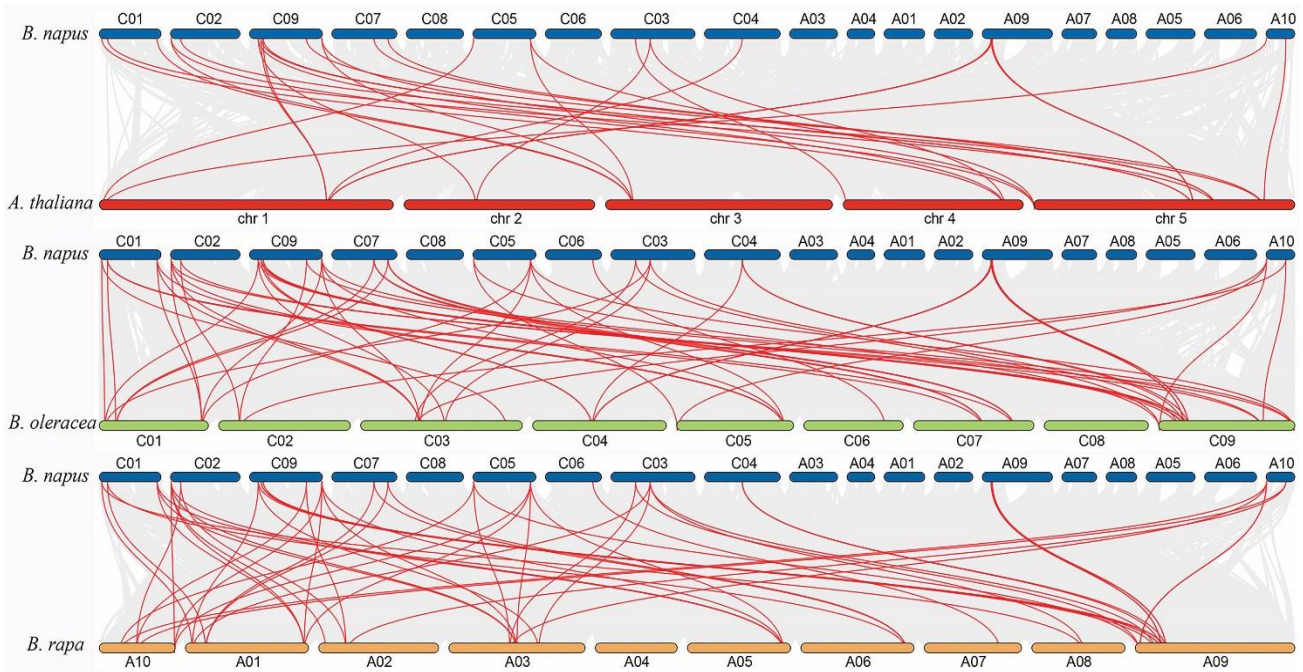


Fig. 6. The collinear relationships of *BnaBSKs* between *A. thaliana*, *B. oleracea*, and *B. rapa*. The collinear BSK gene pairs between the indicated species are shown by red lines. Gray background components denote collinear regions.

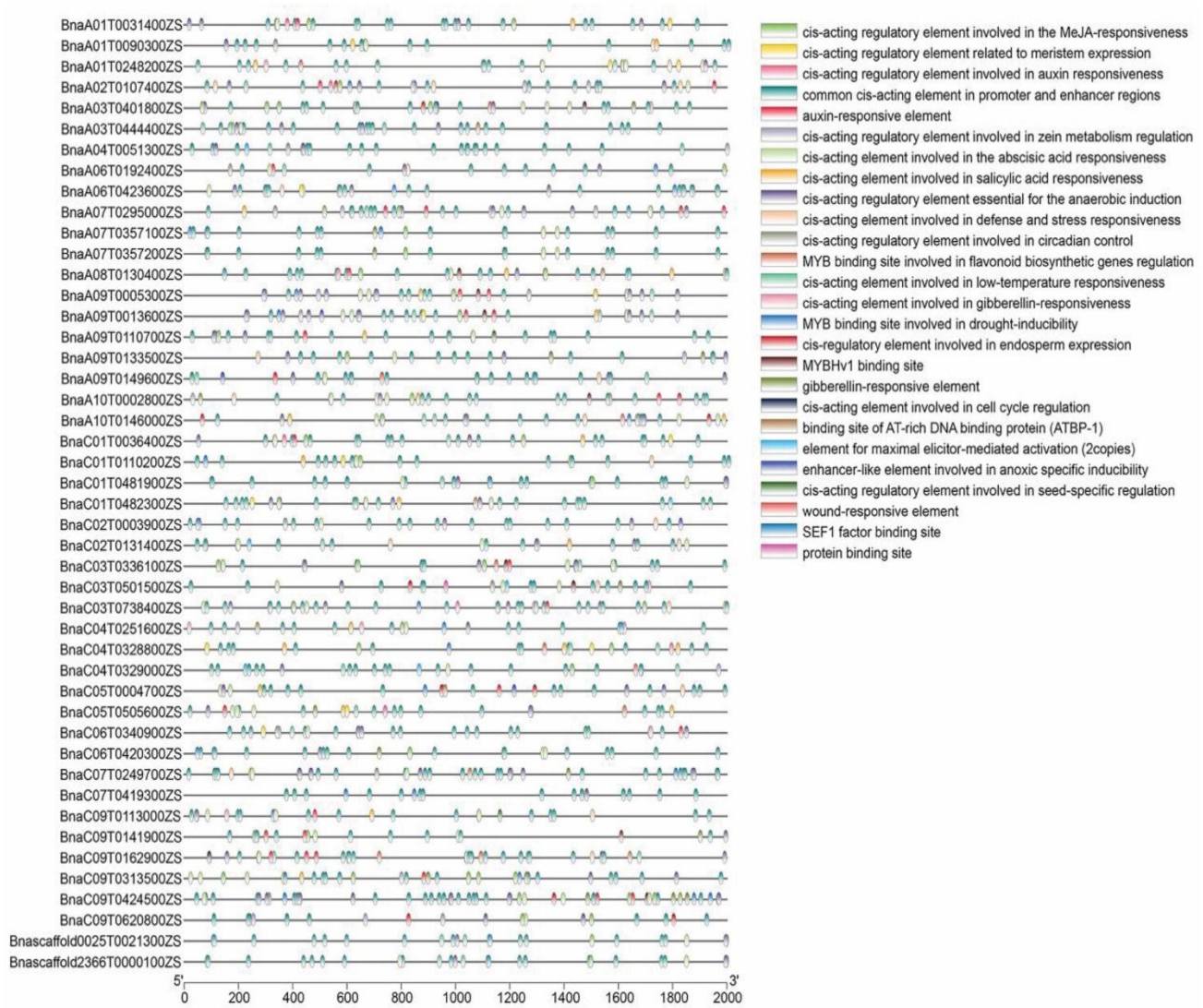


Fig. 7. *Cis*-acting elements in the promoter region of *the BSK* gene family of *B. napus.*

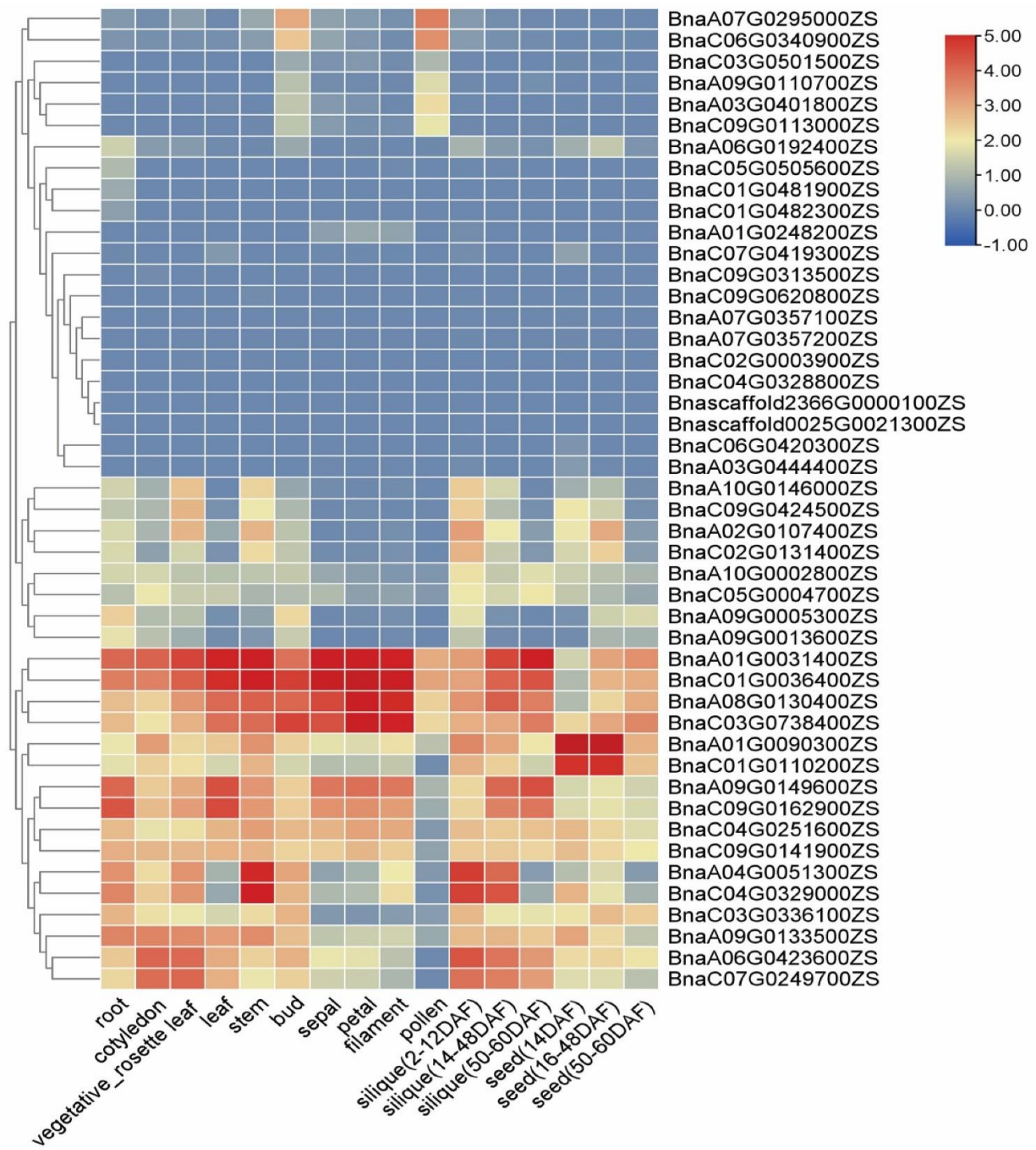


Fig. 8. The expression patterns of *BnaBSKs* in different tissues or organs at various developmental stages in *B. napus*. The heatmap was drawn using TBtools' HeatMap Illustrator (Deng *et al.*, 2014). The colour bar represents the expression values.

**Expression profiles of *BnaBSKs* in various tissues:** To assess the expression patterns of *BnaBSK* genes across tissues and growth phases in *B. napus*, public microarray data sets were analyzed. The findings revealed distinct expression profiles for 46 *BnaBSK* genes in roots, cotyledons, rosette leaves, leaves, stems, buds, sepals, petals, filaments, pollen, siliques, and seeds (Fig. 8). *BnaA01G0031400ZS*, *BnaC01G0036400ZS*, *BnaA08G0130400ZS*, and *BnaC03G0738400ZS* were consistently highly expressed throughout the growth period, indicating their ongoing contribution to the development of *B. napus* (Fig. 8). In contrast, *BnaA01G0090300ZS* and *BnaC01G0110200ZS* showed elevated expression specifically during the 16 to 48 days of seed development, hinting at temporal specificity in their expression patterns. The expression of *BnaA04G0051300ZS* mirrored that of *BnaC04G0329000ZS*, and similarly, the expression of *BnaA09G0149600ZS* paralleled *BnaC09G0162900ZS*, suggesting that genes from the same evolutionary group tended to exhibit correlated expression trends throughout the growth period (Fig. 8). Taken together, the ubiquitous presence of *BnaBSKs* genes had been observed across various tissues of *B. napus* and may be involved in distinct growth and development stages.

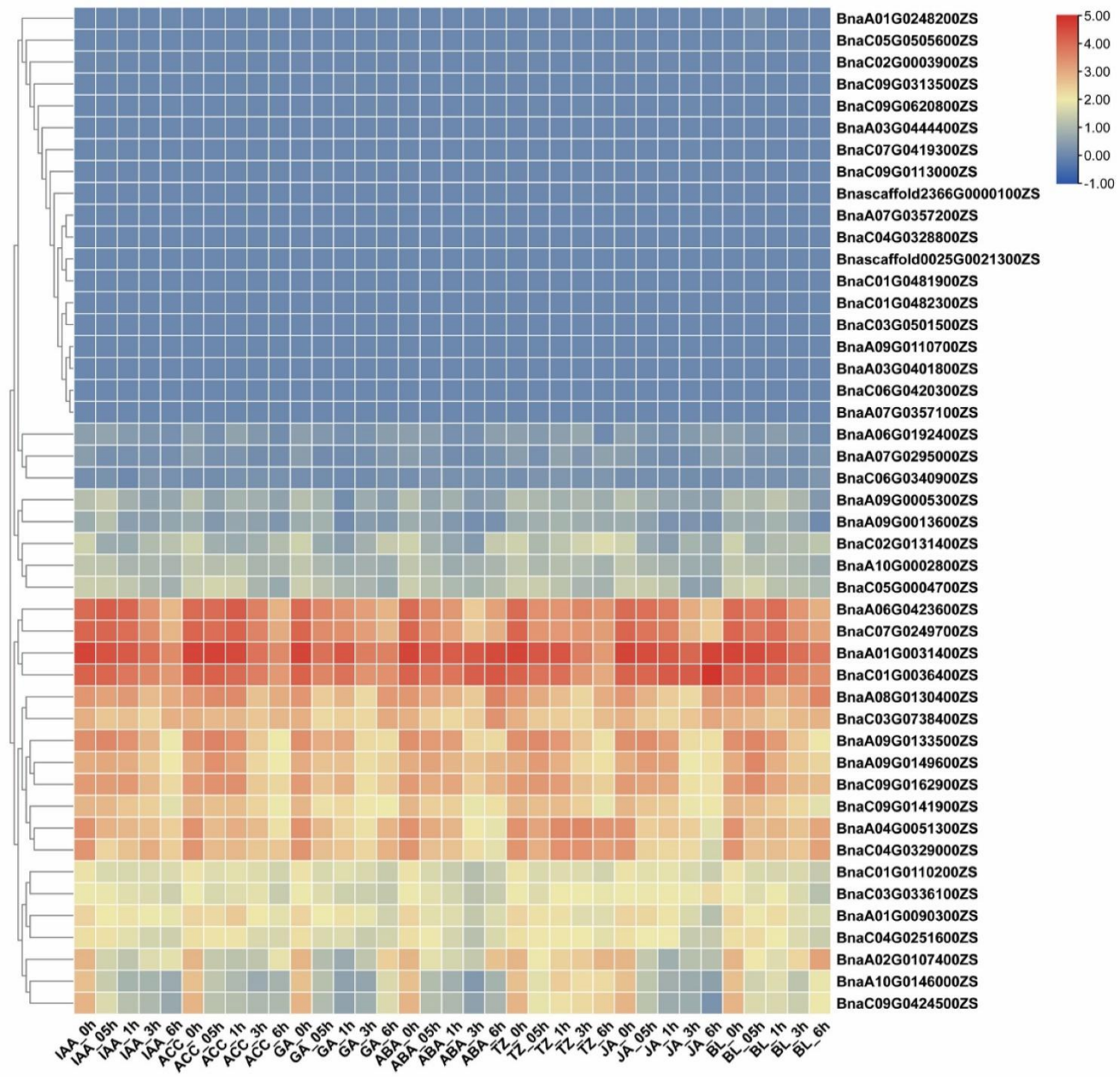


Fig. 9. Hormonal response patterns of *BnaBSKs* genes in *B. napus*. Gene expression heat map in seedling leaves treated with IAA, ACC, gibberellin (GA), abscisic acid (ABA), trans-zeatin (TZ), jasmonate (JA), and brassinolide (BL). The colour bar represents the expression values.

**Expression analysis of *BnaBSKs* genes among hormones and abiotic stress:** To further explore and gain deeper insight into the potential functions of *BnaBSKs* under biotic and abiotic stresses, transcriptome expression data for the *BSK* gene under hormone and abiotic treatment were downloaded from the Huazhong Agricultural University, and the heatmap of *BSK* expression in rapeseed was generated. The expression levels of genes *BnaA06G0423600ZS* and *BnaC07G0 249700ZS* decreased with increasing treatment duration under various hormone treatments; meanwhile, *BnaA01G0031400 ZS* and *BnaC01G0036400ZS* followed suit under all hormone treatments except ABA and JA. However, the expression levels of these 4 genes remained higher than other genes both before and after various hormone treatments. *BnaA04G 0051300ZS* and *BnaC04G0329000ZS*, as well as *BnaA10G0146000ZS* and *BnaC09G0424500ZS*, exhibited similar expression patterns across various hormone treatments. This suggests they may share common functions and potentially interact during hormone responses (Fig. 9).

Under cold stress, the expression of specific genes such as *BnaA04G0051300ZS* and *BnaC04G0329000ZS* peaked at 12 hours and gradually declined over time (Fig. 10). This indicates that these genes may facilitate cold tolerance and response to cold stress. After 12 hours of drought treatment, *BnaA09G0149600ZS* and *BnaC09G 0162900ZS* expression markedly increased, suggesting their potential importance in drought resistance. *BnaC01G0036400ZS* and *BnaA01G00 31400ZS*, as well as *BnaC07G0249700ZS* and *Bna A06G0423600ZS*, exhibited similar responses to various stimuli, displaying comparable expression patterns under different abiotic stress treatments. This was also observed in *BnaC03G0738400ZS* and *BnaA08 G0130400ZS*, suggesting redundant functions in plant resistance to multiple abiotic stresses. These data indicate that *BSK* genes may play a role in mediating plant responses to adversity-induced stress signaling and hormonal adaptation.

**Table S3. Ka, Ks, and Ka/Ks values for the duplication gene pairs from *Brassica napus BSK* family.**

| Seq1 | Seq2 | Ka | Ks | Ka/Ks Ratio | Date (MY) | Duplication type |
|---|---|---|---|---|---|---|
| BnaA01G0031400ZS | BnaA03G0401800ZS | 0.270379596 | 1.28765623 | 0.209978089 | 42.92187447 | WGD or Segmental |
| BnaA01G0031400ZS | BnaA09G0110700ZS | 0.262103129 | 1.42652683 | 0.183735156 | 47.55089417 | WGD or Segmental |
| BnaA01G0031400ZS | BnaC01G0036400ZS | 0.00257235 | 0.12185739 | 0.02110951 | 4.061913 | WGD or Segmental |
| BnaA01G0031400ZS | BnaC03G0501500ZS | 0.25842671 | 1.30826792 | 0.197533476 | 43.60893077 | WGD or Segmental |
| BnaA01G0031400ZS | BnaC09G0113000ZS | 0.252592585 | 1.38230024 | 0.182733517 | 46.0766748 | WGD or Segmental |
| BnaA01G0090300ZS | BnaA03G0444400ZS | 0.215633557 | 0.36162976 | 0.596282661 | 12.05432543 | WGD or Segmental |
| BnaA01G0090300ZS | BnaA06G0423600ZS | 0.078709119 | 0.66304198 | 0.118709104 | 22.10139927 | WGD or Segmental |
| BnaA01G0090300ZS | BnaC01G0110200ZS | 0.014885567 | 0.08203599 | 0.181451669 | 2.734532967 | WGD or Segmental |
| BnaA01G0090300ZS | BnaC07G0419300ZS | 0.201068092 | 0.36923761 | 0.544549333 | 12.3079202 | WGD or Segmental |
| BnaA01G0090300ZS | BnaC07G0249700ZS | 0.078642304 | 0.68096564 | 0.115486449 | 22.6988548 | WGD or Segmental |
| BnaA02G0107400ZS | BnaA10G0146000ZS | 0.025664694 | 0.26152336 | 0.098135377 | 8.717445333 | WGD or Segmental |
| BnaA02G0107400ZS | BnaC02G0131400ZS | 0.002662922 | 0.0976989 | 0.027256415 | 3.256629867 | WGD or Segmental |
| BnaA02G0107400ZS | BnaC09G0424500ZS | 0.026994019 | 0.26386779 | 0.102301306 | 8.795592833 | WGD or Segmental |
| BnaA03G0401800ZS | BnaA09G0110700ZS | 0.139813834 | 0.31540375 | 0.443285257 | 10.51345847 | WGD or Segmental |
| BnaA03G0401800ZS | BnaC01G0036400ZS | 0.271526015 | 1.29421638 | 0.20979955 | 43.14054613 | WGD or Segmental |
| BnaA03G0401800ZS | BnaC03G0501500ZS | 0.02598064 | 0.05801641 | 0.447815404 | 1.9338802 | WGD or Segmental |
| BnaA03G0401800ZS | BnaC09G0113000ZS | 0.135205808 | 0.30223958 | 0.447346463 | 10.07465273 | WGD or Segmental |
| BnaA03G0444400ZS | BnaA06G0423600ZS | 0.221974438 | 0.69511356 | 0.319335502 | 23.1704521 | WGD or Segmental |
| BnaA03G0444400ZS | BnaC01G0110200ZS | 0.220644673 | 0.36538453 | 0.603869775 | 12.1794843 | WGD or Segmental |
| BnaA03G0444400ZS | BnaC07G0419300ZS | 0.017634905 | 0.03583334 | 0.492136805 | 1.194444633 | WGD or Segmental |
| BnaA03G0444400ZS | BnaC07G0249700ZS | 0.222379999 | 0.73600032 | 0.302146607 | 24.5333439 | WGD or Segmental |
| BnaA06G0423600ZS | BnaC01G0110200ZS | 0.080833106 | 0.62747599 | 0.128822629 | 20.91586617 | WGD or Segmental |
| BnaA06G0423600ZS | BnaC07G0419300ZS | 0.211922198 | 0.68274682 | 0.310396465 | 22.75822717 | WGD or Segmental |
| BnaA06G0423600ZS | BnaC07G0249700ZS | 0.001761469 | 0.11779256 | 0.01495399 | 3.9264185 | WGD or Segmental |
| BnaA07G0295000ZS | BnaC06G0340900ZS | 0.016916739 | 0.05891708 | 0.287127932 | 1.963902567 | WGD or Segmental |
| BnaA09G0005300ZS | BnaA10G0002800ZS | 0.158414622 | 0.98495729 | 0.160834001 | 32.83190967 | WGD or Segmental |
| BnaA09G0005300ZS | BnaC03G0336100ZS | 0.037977005 | 0.34214364 | 0.110997255 | 11.4047881 | WGD or Segmental |

**Table S3. (Cont'd.).**

| Seq1 | Seq2 | Ka | Ks | Ka/Ks Ratio | Date (MY) | Duplication type |
|---|---|---|---|---|---|---|
| BnaA09G0005300ZS | BnaC05G0004700ZS | 0.154411536 | 0.9766505 | 0.158103165 | 32.55501677 | WGD or Segmental |
| BnaA09G0110700ZS | BnaC01G0036400ZS | 0.258885031 | 1.5361573 | 0.168527683 | 51.20524343 | WGD or Segmental |
| BnaA09G0110700ZS | BnaC03G0501500ZS | 0.144572476 | 0.30768466 | 0.469872227 | 10.2561553 | WGD or Segmental |
| BnaA09G0110700ZS | BnaC09G0113000ZS | 0.015740104 | 0.03334809 | 0.471994191 | 1.111602933 | WGD or Segmental |
| BnaA09G0133500ZS | BnaA09G0149600ZS | 0.021298916 | 0.22984736 | 0.092665483 | 7.661578567 | WGD or Segmental |
| BnaA09G0133500ZS | BnaC04G0251600ZS | 0.016396584 | 0.2038341 | 0.080440833 | 6.794469867 | WGD or Segmental |
| BnaA09G0133500ZS | BnaC09G0141900ZS | 0.002673601 | 0.08725783 | 0.030640244 | 2.9085942 | WGD or Segmental |
| BnaA09G0133500ZS | BnaC09G0162900ZS | 0.022679179 | 0.24827203 | 0.091348103 | 8.275734333 | WGD or Segmental |
| BnaA09G0149600ZS | BnaC04G0251600ZS | 0.022055345 | 0.27671242 | 0.079704934 | 9.223747367 | WGD or Segmental |
| BnaA09G0149600ZS | BnaC09G0162900ZS | 0.00178811 | 0.11244963 | 0.015901431 | 3.748320867 | WGD or Segmental |
| BnaA09G0149600ZS | BnaC09G0141900ZS | 0.019014146 | 0.2815944 | 0.06752317 | 9.386479933 | WGD or Segmental |
| BnaA10G0002800ZS | BnaC05G0004700ZS | 0.028526762 | 0.07828713 | 0.364386364 | 2.609570967 | WGD or Segmental |
| BnaA10G0146000ZS | BnaC02G0131400ZS | 0.023397218 | 0.2669786 | 0.087637056 | 8.899286533 | WGD or Segmental |
| BnaA10G0146000ZS | BnaC09G0424500ZS | 0.011493319 | 0.10959755 | 0.104868398 | 3.6532515 | WGD or Segmental |
| BnaC01G0036400ZS | BnaC03G0501500ZS | 0.259998944 | 1.30878222 | 0.198657148 | 43.62607413 | WGD or Segmental |
| BnaC01G0036400ZS | BnaC09G0113000ZS | 0.249424157 | 1.48561569 | 0.167892786 | 49.52052287 | WGD or Segmental |
| BnaC01G0110200ZS | BnaC07G0419300ZS | 0.208471029 | 0.36615147 | 0.569357347 | 12.205049 | WGD or Segmental |
| BnaC01G0110200ZS | BnaC07G0249700ZS | 0.080764253 | 0.63020097 | 0.128156347 | 21.00669887 | WGD or Segmental |
| BnaC01G0481900ZS | BnaC05G0505600ZS | 0.076951084 | 0.38733271 | 0.198669211 | 12.9110904 | WGD or Segmental |
| BnaC02G0131400ZS | BnaC09G0424500ZS | 0.022645539 | 0.23795757 | 0.095166288 | 7.931919133 | WGD or Segmental |
| BnaC03G0501500ZS | BnaC09G0113000ZS | 0.137707159 | 0.2850386 | 0.48311758 | 9.501286667 | WGD or Segmental |
| BnaC04G0251600ZS | BnaC09G0141900ZS | 0.015482071 | 0.2035442 | 0.07606245 | 6.7848067 | WGD or Segmental |
| BnaC04G0251600ZS | BnaC09G0162900ZS | 0.023922905 | 0.31231421 | 0.076598837 | 10.4104737 | WGD or Segmental |
| BnaC05G0505600ZS | BnaC09G0620800ZS | 0.185699925 | 1.1077639 | 0.167634931 | 36.9254632 | WGD or Segmental |
| BnaC07G0249700ZS | BnaC07G0419300ZS | 0.212312989 | 0.75328892 | 0.281848019 | 25.1096305 | WGD or Segmental |
| BnaC09G0141900ZS | BnaC09G0162900ZS | 0.020850414 | 0.29029645 | 0.071824555 | 9.676548467 | WGD or Segmental |

**Table S4. Ka, Ks, and Ka/Ks values for the duplication gene pairs among *A. thaliana*, *B. rapa*, *B. oleracea* and *B. napus*.**

| Seq1 | Seq2 | Ka | Ks | Ka/Ks Ratio | Date (MY) | Duplication type |
|---|---|---|---|---|---|---|
| AT4G35230.1 | BnaA01G0031400ZS | 0.021218 | 0.493363 | 0.043007 | 16.44544343 | WGD or Segmental |
| AT4G35230.1 | BnaA03G0401800ZS | 0.269885 | 0.956056 | 0.28229 | 31.86854688 | WGD or Segmental |
| AT4G35230.1 | BnaA09G0110700ZS | 0.261238 | 0.989666 | 0.263966 | 32.98885378 | WGD or Segmental |
| AT4G35230.1 | BnaC01G0036400ZS | 0.021802 | 0.499345 | 0.043662 | 16.6448457 | WGD or Segmental |
| AT4G35230.1 | BnaC03G0501500ZS | 0.270315 | 0.955469 | 0.282913 | 31.84896243 | WGD or Segmental |
| AT4G35230.1 | BnaC09G0113000ZS | 0.251772 | 0.987002 | 0.255088 | 32.90005403 | WGD or Segmental |
| AT5G46570.1 | BnaA01G0090300ZS | 0.075011 | 0.685794 | 0.109378 | 22.8597849 | WGD or Segmental |
| AT5G46570.1 | BnaA03G0444400ZS | 0.217616 | 0.666313 | 0.326597 | 22.21044279 | WGD or Segmental |
| AT5G46570.1 | BnaC01G0110200ZS | 0.079608 | 0.657658 | 0.121048 | 21.92191908 | WGD or Segmental |
| AT5G46570.1 | BnaC07G0249700ZS | 0.024122 | 0.436152 | 0.055306 | 14.53839248 | WGD or Segmental |
| AT5G46570.1 | BnaC07G0419300ZS | 0.205804 | 0.662234 | 0.310772 | 22.07447939 | WGD or Segmental |
| AT4G00710.1 | BnaA09G0005300ZS | 0.050975 | 0.501009 | 0.101745 | 16.70030902 | WGD or Segmental |
| AT4G00710.1 | BnaC03G0336100ZS | 0.039817 | 0.39247 | 0.101453 | 13.08233505 | WGD or Segmental |
| AT1G01740.1 | BnaA09G0005300ZS | 0.130355 | 0.941259 | 0.13849 | 31.37530315 | WGD or Segmental |
| AT1G01740.1 | BnaA10G0002800ZS | 0.116747 | 0.328055 | 0.355876 | 10.93517468 | WGD or Segmental |
| AT1G01740.1 | BnaC05G0004700ZS | 0.116678 | 0.348926 | 0.334392 | 11.63086224 | WGD or Segmental |
| AT5G59010.1 | BnaA02G0107400ZS | 0.03299 | 0.386474 | 0.085361 | 12.88246981 | WGD or Segmental |
| AT5G59010.1 | BnaA10G0146000ZS | 0.027006 | 0.389095 | 0.069406 | 12.96984484 | WGD or Segmental |
| AT5G59010.1 | BnaC02G0131400ZS | 0.029327 | 0.360708 | 0.081304 | 12.02358923 | WGD or Segmental |
| AT5G59010.1 | BnaC09G0424500ZS | 0.026337 | 0.360618 | 0.073034 | 12.02058434 | WGD or Segmental |
| AT3G54030.1 | BnaA04G0051300ZS | 0.039349 | 0.54894 | 0.071681 | 18.29801416 | WGD or Segmental |
| AT1G63500.1 | BnaA09G0133500ZS | 0.026113 | 0.444404 | 0.05876 | 14.81346696 | WGD or Segmental |
| AT1G63500.1 | BnaA09G0149600ZS | 0.020295 | 0.459814 | 0.044136 | 15.32713142 | WGD or Segmental |
| AT1G63500.1 | BnaC04G0251600ZS | 0.025645 | 0.431213 | 0.059473 | 14.3737538 | WGD or Segmental |
| AT1G63500.1 | BnaC09G0141900ZS | 0.026123 | 0.438329 | 0.059597 | 14.61095981 | WGD or Segmental |
| AT1G63500.1 | BnaC09G0162900ZS | 0.022139 | 0.517304 | 0.042797 | 17.24347223 | WGD or Segmental |
| AT5G41260.1 | BnaA09G0133500ZS | 0.064576 | 0.661838 | 0.097571 | 22.06127162 | WGD or Segmental |
| AT5G41260.1 | BnaA09G0149600ZS | 0.061931 | 0.798502 | 0.077559 | 26.616726 | WGD or Segmental |
| AT5G41260.1 | BnaC09G0141900ZS | 0.065076 | 0.693905 | 0.093783 | 23.13015239 | WGD or Segmental |
| AT5G41260.1 | BnaC09G0162900ZS | 0.065019 | 0.889405 | 0.073104 | 29.64684712 | WGD or Segmental |
| AT3G09240.3 | BnaC01G0481900ZS | 0.054179 | 0.414473 | 0.130718 | 13.81578321 | WGD or Segmental |
| AT3G09240.3 | BnaC05G0505600ZS | 0.082484 | 0.467473 | 0.176447 | 15.58244013 | WGD or Segmental |
| AT3G09240.3 | BnaC09G0620800ZS | 0.140296 | 0.81526 | 0.172088 | 27.17533927 | WGD or Segmental |
| AT5G01060.1 | BnaA10G0146000ZS | 0.283887 | 2.194356 | 0.129371 | 73.14520068 | WGD or Segmental |

**Table S4. (Cont'd.).**

| Seq1 | Seq2 | Ka | Ks | Ka/Ks Ratio | Date (MY) | Duplication type |
|---|---|---|---|---|---|---|
| AT5G01060.1 | BnaC05G0505600ZS | 0.155862 | 0.987816 | 0.157784 | 32.92719863 | WGD or Segmental |
| AT5G01060.1 | BnaC09G0620800ZS | 0.085876 | 0.477442 | 0.179867 | 15.91473743 | WGD or Segmental |
| AT5G01060.1 | BnaC09G0424500ZS | 0.277966 | 4.878302 | 0.05698 | 162.610083 | WGD or Segmental |
| AT2G17090.1 | BnaA01G0031400ZS | 0.258494 | 1.266385 | 0.20412 | 42.21282798 | WGD or Segmental |
| AT2G17090.1 | BnaA03G0401800ZS | 0.205314 | 0.512642 | 0.400502 | 17.08806168 | WGD or Segmental |
| AT2G17090.1 | BnaA09G0110700ZS | 0.194999 | 0.52027 | 0.374804 | 17.34233698 | WGD or Segmental |
| AT2G17090.1 | BnaC01G0036400ZS | 0.254511 | 1.203126 | 0.211541 | 40.1041952 | WGD or Segmental |
| AT2G17090.1 | BnaC03G0501500ZS | 0.197963 | 0.499261 | 0.396512 | 16.64203962 | WGD or Segmental |
| AT2G17090.1 | BnaC09G0113000ZS | 0.188704 | 0.503394 | 0.374863 | 16.77980261 | WGD or Segmental |
| BolC01g003670.2J.ml | BnaA01G0031400ZS | 0.005154 | 0.128674 | 0.040051 | 4.289122738 | WGD or Segmental |
| BolC03g078900.2J.ml | BnaA01G0031400ZS | 0.027659 | 0.347997 | 0.07948 | 11.59991103 | WGD or Segmental |
| BolC01g011540.2J.ml | BnaA01G0090300ZS | 0.007838 | 0.075595 | 0.103685 | 2.519833743 | WGD or Segmental |
| BolC07g047430.2J.ml | BnaA01G0090300ZS | 0.188549 | 0.364272 | 0.517604 | 12.14240453 | WGD or Segmental |
| BolC07g029130.2J.ml | BnaA01G0090300ZS | 0.078642 | 0.673456 | 0.116774 | 22.44853983 | WGD or Segmental |
| BolC02g013850.2J.ml | BnaA02G0107400ZS | 0.002663 | 0.101019 | 0.026364 | 3.367309076 | WGD or Segmental |
| BolC09g047990.2J.ml | BnaA02G0107400ZS | 0.028854 | 0.264487 | 0.109094 | 8.816248529 | WGD or Segmental |
| BolC01g003670.2J.ml | BnaA03G0401800ZS | 0.27285 | 1.294216 | 0.210822 | 43.14054615 | WGD or Segmental |
| BolC03g052690.2J.ml | BnaA03G0401800ZS | 0.024596 | 0.054208 | 0.453743 | 1.80692708 | WGD or Segmental |
| BolC03g078900.2J.ml | BnaA03G0401800ZS | 0.289444 | 1.091668 | 0.26514 | 36.38891845 | WGD or Segmental |
| BolC09g012390.2J.ml | BnaA03G0401800ZS | 0.135206 | 0.30224 | 0.447346 | 10.07465274 | WGD or Segmental |
| BolC01g011540.2J.ml | BnaA03G0444400ZS | 0.216595 | 0.356899 | 0.606881 | 11.89662608 | WGD or Segmental |
| BolC07g047430.2J.ml | BnaA03G0444400ZS | 0.034711 | 0.058539 | 0.592954 | 1.951297262 | WGD or Segmental |
| BolC07g029130.2J.ml | BnaA03G0444400ZS | 0.22238 | 0.7275 | 0.305677 | 24.24998787 | WGD or Segmental |
| BolC04g038220.2J.ml | BnaA04G0051300ZS | 0.008868 | 0.140474 | 0.063129 | 4.682479197 | WGD or Segmental |
| BolC01g011540.2J.ml | BnaA06G0423600ZS | 0.073917 | 0.623964 | 0.118464 | 20.79878594 | WGD or Segmental |
| BolC07g047430.2J.ml | BnaA06G0423600ZS | 0.201112 | 0.684851 | 0.293658 | 22.82837899 | WGD or Segmental |
| BolC07g029130.2J.ml | BnaA06G0423600ZS | 0.001761 | 0.11074 | 0.015906 | 3.691330089 | WGD or Segmental |
| BolC06g038900.2J.ml | BnaA07G0295000ZS | 0.006331 | 0.072664 | 0.087128 | 2.422134918 | WGD or Segmental |
| BolC03g035330.2J.ml | BnaA09G0005300ZS | 0.04316 | 0.377132 | 0.114442 | 12.57105606 | WGD or Segmental |
| BolC05g000280.2J.ml | BnaA09G0005300ZS | 0.179283 | 0.996056 | 0.179993 | 33.20185217 | WGD or Segmental |
| BolC09g000490.2J.ml | BnaA09G0005300ZS | 0.018774 | 0.248412 | 0.075575 | 8.280399568 | WGD or Segmental |
| BolC01g003670.2J.ml | BnaA09G0110700ZS | 0.261498 | 1.511481 | 0.173008 | 50.3826881 | WGD or Segmental |
| BolC03g052690.2J.ml | BnaA09G0110700ZS | 0.141951 | 0.302688 | 0.468968 | 10.08961141 | WGD or Segmental |
| BolC09g012390.2J.ml | BnaA09G0110700ZS | 0.01574 | 0.033348 | 0.471994 | 1.111602945 | WGD or Segmental |

**Table S4. (Cont'd.).**

| Seq1 | Seq2 | Ka | Ks | Ka/Ks Ratio | Date (MY) | Duplication type |
|---|---|---|---|---|---|---|
| BolC04g029650.2J.ml | BnaA09G0133500ZS | 0.016397 | 0.203834 | 0.080441 | 6.79446986 | WGD or Segmental |
| BolC09g015310.2J.ml | BnaA09G0133500ZS | 0.002674 | 0.08396 | 0.031844 | 2.798673713 | WGD or Segmental |
| BolC09g017580.2J.ml | BnaA09G0133500ZS | 0.020833 | 0.240308 | 0.086693 | 8.010279894 | WGD or Segmental |
| BolC04g029650.2J.ml | BnaA09G0149600ZS | 0.022055 | 0.276712 | 0.079705 | 9.223747378 | WGD or Segmental |
| BolC09g017580.2J.ml | BnaA09G0149600ZS | 0 | 0.109108 | 0 | 3.636939964 | WGD or Segmental |
| BolC09g015310.2J.ml | BnaA09G0149600ZS | 0.020388 | 0.292665 | 0.069663 | 9.75550402 | WGD or Segmental |
| BolC05g000280.2J.ml | BnaA10G0002800ZS | 0.027595 | 0.066418 | 0.415465 | 2.213948992 | WGD or Segmental |
| BolC09g000490.2J.ml | BnaA10G0002800ZS | 0.152527 | 1.212376 | 0.125808 | 40.41253785 | WGD or Segmental |
| BolC02g013850.2J.ml | BnaA10G0146000ZS | 0.023401 | 0.271049 | 0.086334 | 9.034968788 | WGD or Segmental |
| BolC09g047990.2J.ml | BnaA10G0146000ZS | 0.00842 | 0.102765 | 0.081936 | 3.425501889 | WGD or Segmental |
| BolC01g003670.2J.ml | BnaC01G0036400ZS | 0.002571 | 0.005797 | 0.44357 | 0.193237677 | WGD or Segmental |
| BolC03g078900.2J.ml | BnaC01G0036400ZS | 0.025462 | 0.347506 | 0.073269 | 11.58353287 | WGD or Segmental |
| BolC01g011540.2J.ml | BnaC01G0110200ZS | 0.006975 | 0.005982 | 1.165942 | 0.199402852 | WGD or Segmental |
| BolC07g047430.2J.ml | BnaC01G0110200ZS | 0.195803 | 0.361236 | 0.542036 | 12.04120022 | WGD or Segmental |
| BolC07g029130.2J.ml | BnaC01G0110200ZS | 0.080764 | 0.61632 | 0.131043 | 20.54399045 | WGD or Segmental |
| BolC01g052980.2J.ml | BnaC01G0481900ZS | 0.003918 | 0.135073 | 0.029005 | 4.502421544 | WGD or Segmental |
| BolC03g039810.2J.ml | BnaC01G0481900ZS | 0.0804 | 0.299218 | 0.268699 | 9.97391855 | WGD or Segmental |
| BolC05g057130.2J.ml | BnaC01G0481900ZS | 0.078052 | 0.386907 | 0.201734 | 12.89690349 | WGD or Segmental |
| BolC02g013850.2J.ml | BnaC02G0131400ZS | 0.001776 | 0.002951 | 0.601746 | 0.09837691 | WGD or Segmental |
| BolC09g047990.2J.ml | BnaC02G0131400ZS | 0.026581 | 0.25317 | 0.104994 | 8.438987889 | WGD or Segmental |
| BolC03g035330.2J.ml | BnaC03G0336100ZS | 0.001919 | 0.054279 | 0.035362 | 1.80929994 | WGD or Segmental |
| BolC09g000490.2J.ml | BnaC03G0336100ZS | 0.019112 | 0.318424 | 0.060021 | 10.61413199 | WGD or Segmental |
| BolC01g003670.2J.ml | BnaC03G0501500ZS | 0.261305 | 1.308782 | 0.199655 | 43.62607415 | WGD or Segmental |
| BolC03g052690.2J.ml | BnaC03G0501500ZS | 0.005831 | 0.006926 | 0.841903 | 0.230881872 | WGD or Segmental |
| BolC03g078900.2J.ml | BnaC03G0501500ZS | 0.27536 | 1.059825 | 0.259817 | 35.32749527 | WGD or Segmental |
| BolC09g012390.2J.ml | BnaC03G0501500ZS | 0.137707 | 0.285039 | 0.483118 | 9.50128667 | WGD or Segmental |
| BolC04g029650.2J.ml | BnaC04G0251600ZS | 0 | 0 | NaN | 0 | WGD or Segmental |
| BolC09g015310.2J.ml | BnaC04G0251600ZS | 0.015482 | 0.207452 | 0.07463 | 6.915057718 | WGD or Segmental |
| BolC09g017580.2J.ml | BnaC04G0251600ZS | 0.022049 | 0.299133 | 0.073708 | 9.97109521 | WGD or Segmental |
| BolC05g000280.2J.ml | BnaC05G0004700ZS | 0.005853 | 0.011842 | 0.494205 | 0.394745043 | WGD or Segmental |
| BolC09g000490.2J.ml | BnaC05G0004700ZS | 0.127678 | 1.093208 | 0.116792 | 36.44025285 | WGD or Segmental |
| BolC01g052980.2J.ml | BnaC05G0505600ZS | 0.079785 | 0.392541 | 0.203252 | 13.08471508 | WGD or Segmental |
| BolC03g039810.2J.ml | BnaC05G0505600ZS | 0.11084 | 0.371501 | 0.298356 | 12.38335533 | WGD or Segmental |
| BolC05g057130.2J.ml | BnaC05G0505600ZS | 0.001757 | 0.006023 | 0.291748 | 0.200753902 | WGD or Segmental |

**Table S4. (Cont'd.).**

| Seq1 | Seq2 | Ka | Ks | Ka/Ks Ratio | Date (MY) | Duplication type |
|---|---|---|---|---|---|---|
| BolC09g069390.2J.ml | BnaC05G0505600ZS | 0.189145 | 1.1458 | 0.165077 | 38.19333983 | WGD or Segmental |
| BolC06g038900.2J.ml | BnaC06G0340900ZS | 0.018 | 0.059786 | 0.30108 | 1.992869089 | WGD or Segmental |
| BolC01g011540.2J.ml | BnaC07G0249700ZS | 0.073855 | 0.633706 | 0.116544 | 21.12351896 | WGD or Segmental |
| BolC07g029130.2J.ml | BnaC07G0249700ZS | 0 | 0.018444 | 0 | 0.614785078 | WGD or Segmental |
| BolC07g047430.2J.ml | BnaC07G0249700ZS | 0.201506 | 0.755664 | 0.266661 | 25.18880808 | WGD or Segmental |
| BolC01g011540.2J.ml | BnaC07G0419300ZS | 0.201339 | 0.357606 | 0.56302 | 11.92020917 | WGD or Segmental |
| BolC07g047430.2J.ml | BnaC07G0419300ZS | 0.009425 | 0.006145 | 1.533722 | 0.20483523 | WGD or Segmental |
| BolC07g029130.2J.ml | BnaC07G0419300ZS | 0.212313 | 0.745034 | 0.284971 | 24.83446149 | WGD or Segmental |
| BolC01g003670.2J.ml | BnaC09G0113000ZS | 0.252001 | 1.462418 | 0.172318 | 48.74726535 | WGD or Segmental |
| BolC03g052690.2J.ml | BnaC09G0113000ZS | 0.134695 | 0.278775 | 0.483166 | 9.292484562 | WGD or Segmental |
| BolC09g012390.2J.ml | BnaC09G0113000ZS | 0 | 0 | NaN | 0 | WGD or Segmental |
| BolC04g029650.2J.ml | BnaC09G0141900ZS | 0.015482 | 0.203544 | 0.076062 | 6.784806691 | WGD or Segmental |
| BolC09g015310.2J.ml | BnaC09G0141900ZS | 0 | 0.008867 | 0 | 0.295569945 | WGD or Segmental |
| BolC09g017580.2J.ml | BnaC09G0141900ZS | 0.019008 | 0.299465 | 0.063475 | 9.982172745 | WGD or Segmental |
| BolC04g029650.2J.ml | BnaC09G0162900ZS | 0.023923 | 0.312314 | 0.076599 | 10.41047369 | WGD or Segmental |
| BolC09g017580.2J.ml | BnaC09G0162900ZS | 0.001788 | 0.046192 | 0.038699 | 1.539737433 | WGD or Segmental |
| BolC09g015310.2J.ml | BnaC09G0162900ZS | 0.021767 | 0.294865 | 0.07382 | 9.828817855 | WGD or Segmental |
| BolC02g013850.2J.ml | BnaC09G0424500ZS | 0.023904 | 0.242944 | 0.098393 | 8.098133888 | WGD or Segmental |
| BolC09g047990.2J.ml | BnaC09G0424500ZS | 0.006019 | 0.004027 | 1.494788 | 0.13422851 | WGD or Segmental |
| BolC01g052980.2J.ml | BnaC09G0620800ZS | 0.157191 | 1.012336 | 0.155276 | 33.74453776 | WGD or Segmental |
| BolC03g039810.2J.ml | BnaC09G0620800ZS | 0.183517 | 0.967921 | 0.189599 | 32.26402188 | WGD or Segmental |
| BolC05g057130.2J.ml | BnaC09G0620800ZS | 0.184278 | 1.135921 | 0.162228 | 37.8640481 | WGD or Segmental |
| BolC09g069390.2J.ml | BnaC09G0620800ZS | 0.004378 | 0.018368 | 0.238362 | 0.6122755 | WGD or Segmental |
| BraA01g003170.3C.1 | BnaA01G0031400ZS | 0.053335 | 0.19098 | 0.27927 | 6.365996167 | WGD or Segmental |
| BraA01g003170.3C.1 | BnaA03G0401800ZS | 0.315566 | 1.155964 | 0.27299 | 38.5321256 | WGD or Segmental |
| BraA09g000440.3C.1 | BnaA09G0005300ZS | 0.012791 | 0.084708 | 0.151004 | 2.8236004 | WGD or Segmental |
| BraA01g003170.3C.1 | BnaA09G0110700ZS | 0.296673 | 1.348189 | 0.220053 | 44.9396384 | WGD or Segmental |
| BraA09g000440.3C.1 | BnaA10G0002800ZS | 0.156629 | 0.960169 | 0.163126 | 32.0056309 | WGD or Segmental |
| BraA09g000440.3C.1 | BnaA10G0002800ZS | 0.156629 | 0.960169 | 0.163126 | 32.0056309 | WGD or Segmental |
| BraA01g003170.3C.1 | BnaC01G0036400ZS | 0.052878 | 0.201698 | 0.262166 | 6.723263233 | WGD or Segmental |
| BraA09g000440.3C.1 | BnaC03G0336100ZS | 0.023685 | 0.303172 | 0.078124 | 10.10572153 | WGD or Segmental |
| BraA01g003170.3C.1 | BnaC03G0501500ZS | 0.302514 | 1.174757 | 0.257512 | 39.15856557 | WGD or Segmental |
| BraA09g000440.3C.1 | BnaC05G0004700ZS | 0.13236 | 0.944804 | 0.140093 | 31.49346593 | WGD or Segmental |
| BraA01g003170.3C.1 | BnaC09G0113000ZS | 0.285705 | 1.312421 | 0.217693 | 43.74735387 | WGD or Segmental |

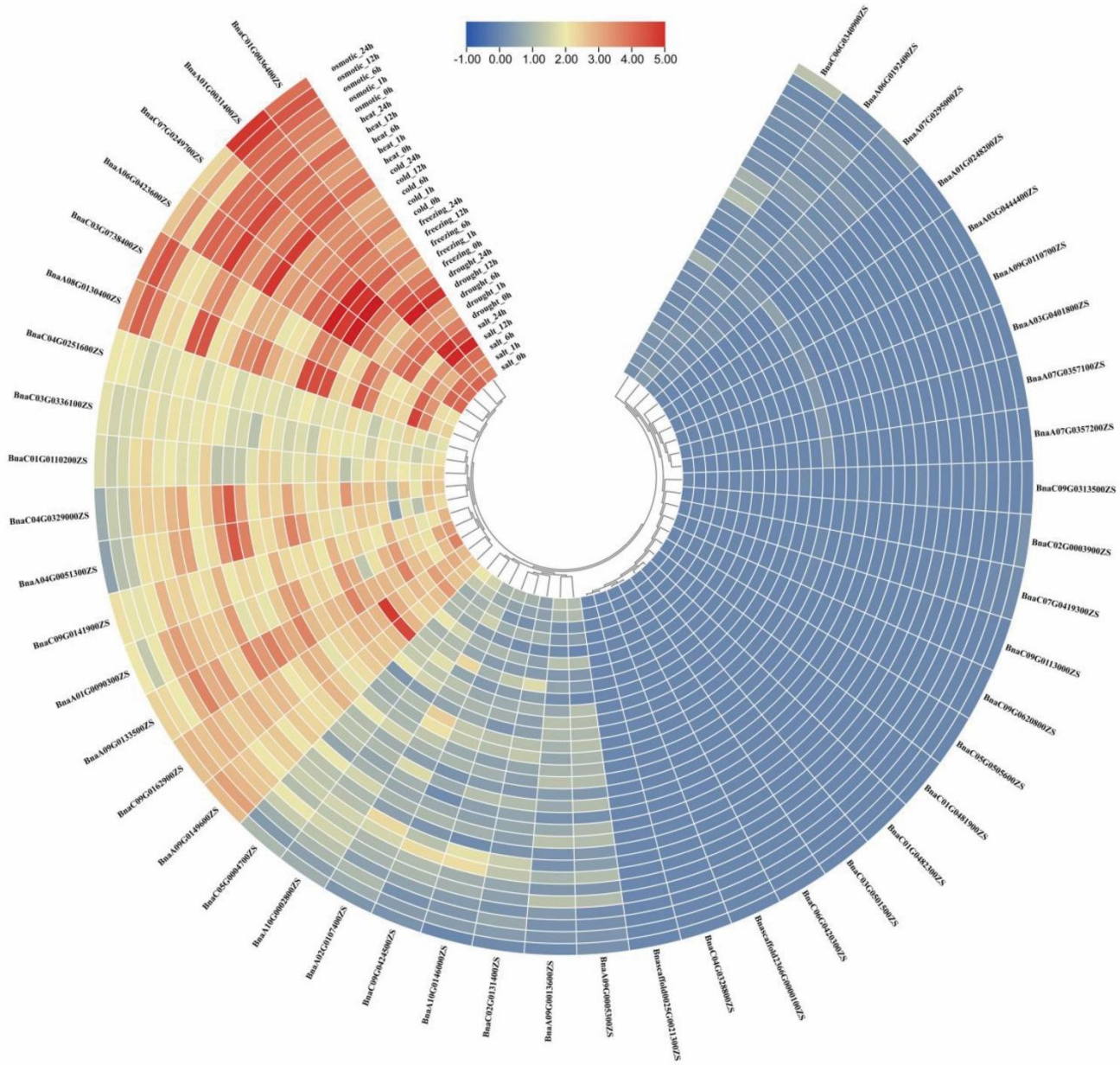


Fig. 10. *BnaBSKs* gene expression patterns in *B. napus* under abiotic stress. Heat map representation of the *BSK* genes across six stress conditions, namely, salt, drought, freezing, cold, heat, and osmotic. Different colors represent different expression values.

**Expression profile of *BnaBSK* in *B. napus* in response to NaCl and PEG:** To investigate the expression patterns of *BSK* genes in *B. napus* under drought and salt stress, we selected two categories of genes for RT-qPCR analysis: first, genes significantly upregulated under drought treatment with promoters rich in drought response elements, including *BnaA09G0149600ZS* and *BnaC09G0162900ZS*. Second, genes constitutively highly expressed in all tissues and stably or up-regulated under most stress treatments, potentially representing core members of fundamental signaling pathways, including *BnaA01G0031400ZS*, *BnaC01G0036400ZS*, *BnaC07G0249700ZS*, and *BnaA06G0423600ZS*. Our analysis revealed differential responsiveness of the six *BnaBSK* genes to drought and salt stress (Fig. 11). Compared with the 0 h control, at 3 h after drought treatment, the expression of *BnaA01G0031400ZS* and *BnaC01G0036400ZS* was rapidly induced and significantly upregulated, while *BnaC07G0249700ZS* and *BnaA06G0423600ZS* were markedly downregulated. No significant expression changes were observed for *BnaA09G0149600ZS* or *BnaC09G0162900ZS* at this time point. After 12 h of salt treatment, *BnaA06G0423600ZS*, *BnaA09G0149600ZS*, and *BnaC09G0162900ZS* were significantly upregulated, *BnaA01G0031400ZS* was downregulated, and *BnaC01G0036400ZS* and *BnaC07G0249700ZS* maintained baseline expression levels. Comparison of expression trends showed that under PEG-induced drought treatment, only *BnaC07G0249700ZS* and *BnaA06G0423600ZS* exhibited expression patterns largely consistent with the transcriptomic data. Under salt treatment, *BnaA09G0149600ZS* and *BnaC09G0162900ZS* matched the trends observed in the transcriptome. During PEG treatment, *BnaA01G0031400ZS* and *BnaC01G0036400ZS* showed the greatest magnitude of upregulation, whereas under salt stress, *BnaC07G0249700ZS* and *BnaA06G0423600ZS* displayed the most pronounced changes in expression level. These results provide a valuable reference for future functional studies on salt- and drought-responsive genes in *B. napus*.

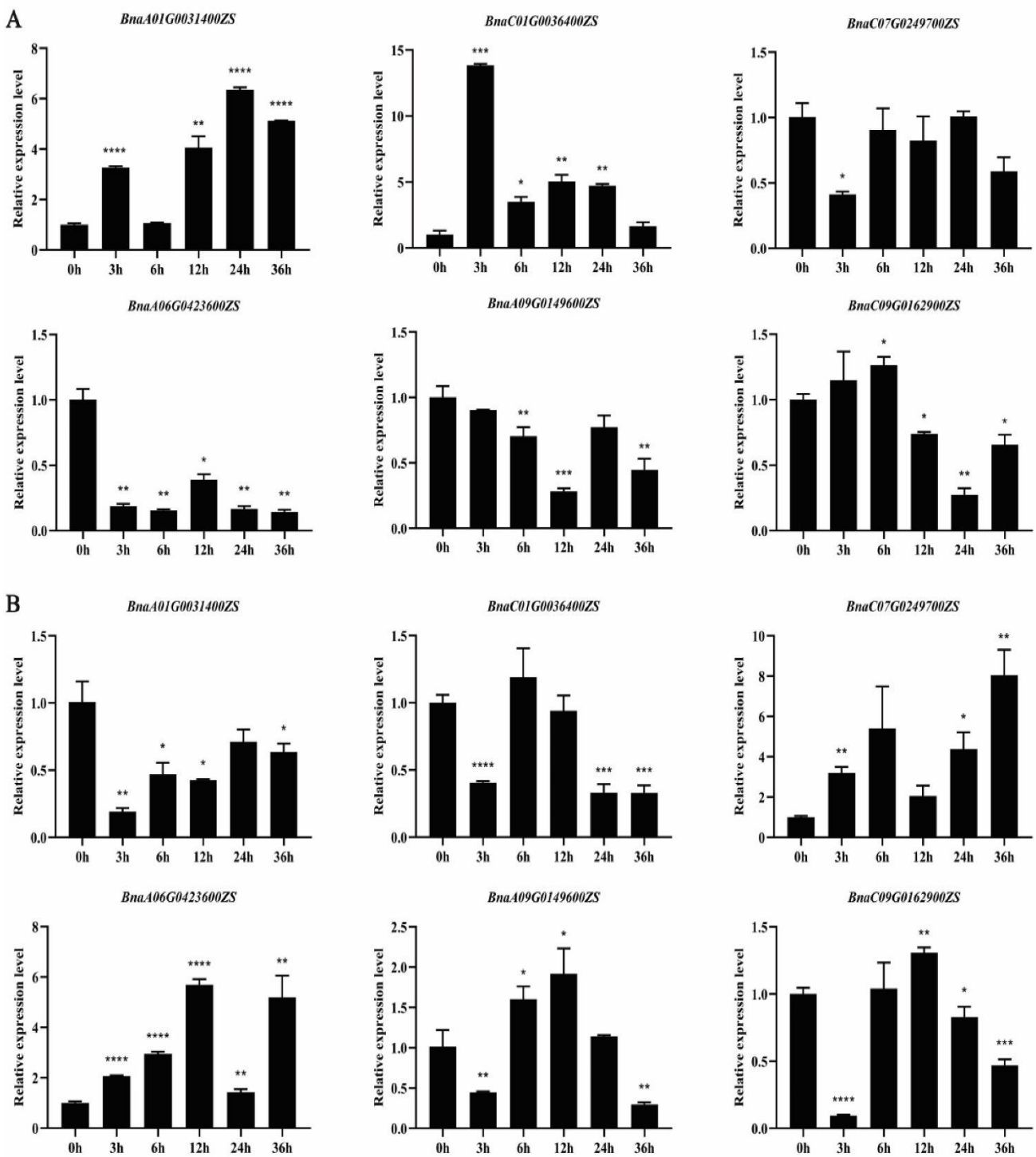


Fig. 11. Expression levels of six *BnaBSKs* under PEG and salt treatments. The mean of three biological replicates was used as the height of the bar graph. Asterisks on the bar show significant difference at **p*<0.05, ***p*<0.01, ****p*<0.001, *****p*<0.0001. (A) Expression of six *BnaBSK* genes after 0 h, 3 h, 6 h, 12 h, 24 h, and 36 h under PEG treatment. (B) Expression of six *BnaBSK* genes after 0 h, 3 h, 6 h, 12 h, 24 h, and 36 h under salt treatment.

**Table S5. Primer used for Real time PCR analysis.**

| Gene names | Sense Primer (5'-3') | Anti-sense Primer (5'-3') |
|---|---|---|
| BnaA01G0031400ZS | CGAAGGAAAATTCTCAACGGAA | TGCCTCATCGTGCTTCTTTATTC |
| BnaC01G0036400ZS | AAACCGCCATAGACTGTTACTCA | CGTCTGGTTGATCGCATAGTAAGT |
| BnaC07G0249700ZS | CTTTTAGATCTTTTAAGCGGCAAA | TCCATCAAAAGCAATGCGTTCT |
| BnaA06G0423600ZS | CTTTTAGATCTTTTAAGCGGCAAA | ATGAATCCATCAATAGCAACGC |
| BnaA09G0149600ZS | TGACGGGACTGAACTAATACGG | TGTTGAGGCACTGCTTGGTATT |
| BnaC09G0162900ZS | TGACGGGACTGAACTCATACGG | TGTTGAGGCACTGCTTGGTATT |

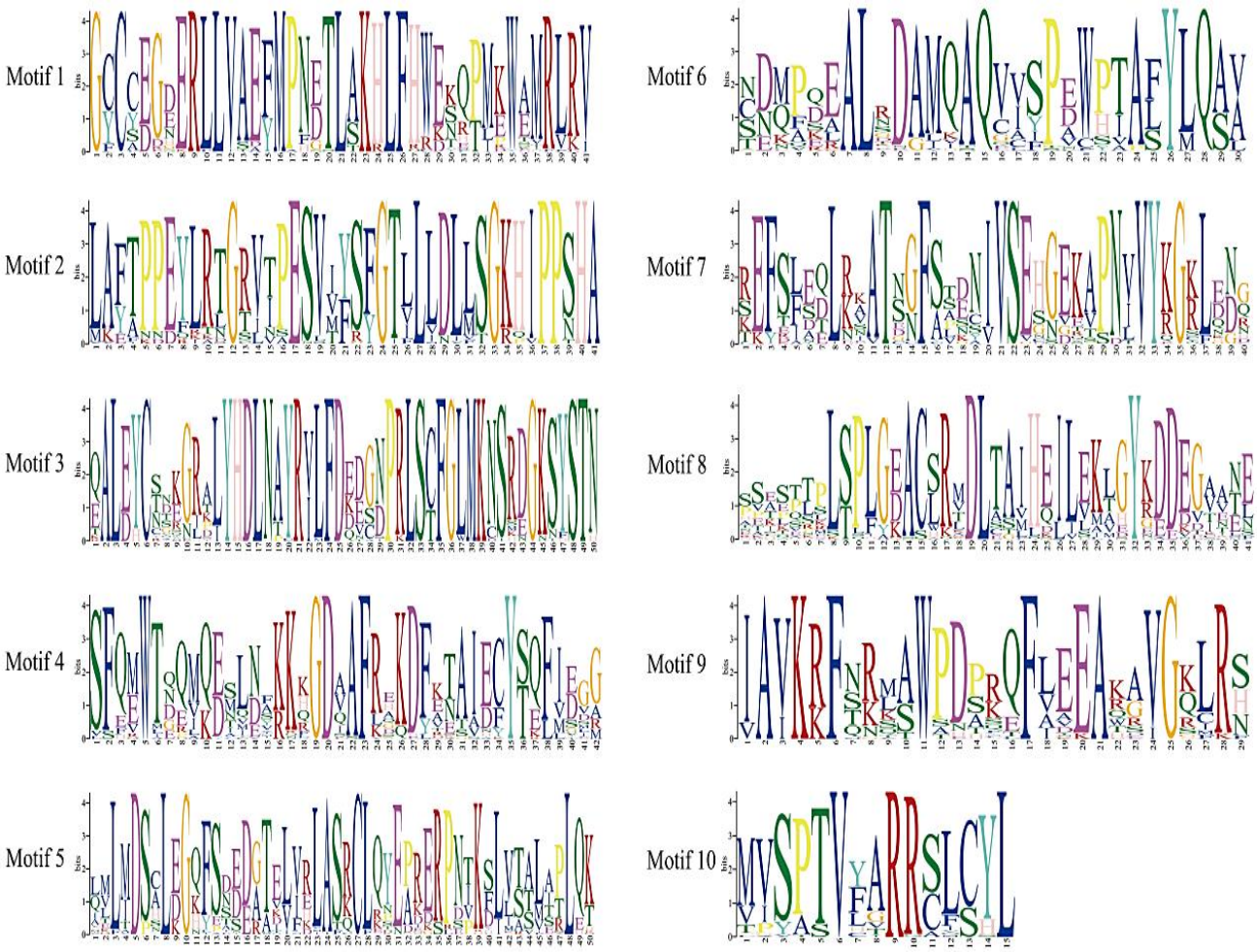


Fig. S1. Conserved Motif-Logo graphs.

**Discussions**

Although numerous studies have been conducted on the BR signaling pathway and its molecular players, the evolutionary origins and diverse roles of *BSK* genes in *B. napus* remain underexplored. *B. napus*, commonly cultivated as rapeseed, holds global significance as a premier oilseed crop, with the *BSK* gene family essential for its growth, development, and stress adaptation. The systematic characterization of *BSK* genes in *B. napus* provides new insights into their evolution, structure, and functions. The diverse expression patterns and *cis*-element profiles suggest multifaceted effects on growth regulation, developmental processes, and stress adaptation. These findings lay a foundation for further genetic manipulation to improve crop performance.

The extensive investigation on the brassinosteroid signaling kinase gene family in *B. napus* has revealed novel insights into their intricate evolutionary history, structural diversity, and multifaceted functional responsibilities. The analysis not only extends findings from model plants like *A. thaliana*, but also reveals specific adaptations and complexities within *B. napus*.

First, phylogenetic analysis underscores the dynamic nature of gene families during polyploidy and hybridization events, which have shaped the evolutionary landscape of *B. napus*. In the phylogenetic tree of BSK in *Arabidopsis*, AtBSK3, AtBSK4, AtBSK7, and AtBSK8 are clustered within the same branch. This branch appears to be functionally important, particularly in mediating BR signaling (Shi *et al.*, 2024). Phylogenetic analysis grouped 89 *BSK* genes from *B. napus*, *B. rapa*, and *B. oleracea* into eight distinct clades, highlighting conserved and divergent evolutionary patterns (Fig. 2). For example, the *B. napus* genes *BnaA08G0130400ZS* and *BnaC03G0738400ZS* are classified within the seventh group alongside the *A. thaliana* gene *AT4G35230*. These genes exhibit homology with *A. thaliana BSK1*, which is potentially involved in pattern-triggered immunity (PTI) regulation (Zhao *et al.*, 2019). This suggests that, while some *BSK* members may retain ancestral functions (Wang *et al.*, 2024), others have probably undergone functional specialization through genetic drift and selection pressures.

Analysis of protein motifs and domains and gene structure reveals a remarkable degree of variation among *BnaBSK* genes (Fig. 3). Variation in exon-intron structures, differences in the positioning of protein motifs as well as the presence of additional or missing domains in certain proteins, implies potential functional divergence within the family. The PKc and TPR domains mediate signal transduction and protein-protein interactions, respectively (Zeytuni & Zarivach, 2012; Zhang *et al.*, 2016; Lei *et al.*, 2023). Notably, two *B. napus* members, Bna A03G0444400ZS and BnaC07G0419300ZS, unusually possess two PKc kinase catalytic domains, which is a rare feature within the BSK family (Fig. 3). This structural peculiarity, possibly arising

from an intragenic duplication event, may imply dual phosphorylation capability, enabling simultaneous or sequential phosphorylation of multiple downstream substrates and potentially enhancing signal transduction intensity or specificity. Furthermore, duplicated PKc domains might regulate kinase activity through interdomain interactions or allow participation in multiple signaling pathways, such as crosstalk between BR signaling and immune responses. Future investigations involving *In vitro* kinase assays and *In vivo* genetic complementation could validate whether these proteins exhibit enhanced phosphorylation activity or broader substrate specificity. These findings reinforce the importance of these domains in mediating *BSK* functions and highlight potential regulatory mechanisms (Wang *et al.*, 2024).

Chromosome localization and collinearity analysis provide evidence for large-scale duplication events that have driven the functional diversification among *BSK* family genes in *B. napus* (Fig. 4-6). This observation aligns with the allopolyploid origin of *B. napus*, where genome doubling and subsequent chromosomal rearrangements have driven the evolution of novel traits and complexity. The identification of homologous genes with rounds of genome-wide replication suggests that gene duplication and neofunctionalization may have played a role in adapting *B. napus* to diverse environmental conditions (Wang *et al.*, 2020; Lei *et al.*, 2023).

The *cis*-element analysis of the *BnaBSK* gene promoters uncovers a rich repertoire of regulatory elements related to various hormonal signals, developmental processes, and stress responses. The abundance of hormone-related elements, particularly methyl jasmonate, auxin, and abscisic acid, suggests that *BSKs* are intricately linked to hormonal crosstalk and fine-tune plant growth and development (Fig. 7). The presence of drought- and anoxia-linked *cis*-regulatory elements also suggests their potential involvement in mediating stress responses, which are crucial for crop survival and yield under adverse conditions (Huang *et al.*, 2023; Tian *et al.*, 2023; Yan *et al.*, 2025).

The distinct expression patterns of *BnaBSK* genes across diverse tissues and growth phases further emphasize their multifaceted functions. Some genes, such as *BnaA01G0031400ZS* and *BnaC01G0036400ZS*, show continuous high expression throughout growth, highlighting their pivotal participation in maintaining fundamental cellular processes (Chen *et al.*, 2024). On the contrary, genes with tissue- or time-specific expression patterns suggest that *BSKs* are fine-tuned to regulate specific developmental stages or organ-specific functions (Fig. 8). In the study, although gene expression patterns varied, the expression of BnaBSK proteins with similar phylogenetic evolution remained largely consistent across different tissues and organs. For instance, *BnaA04G0051300ZS* and *BnaC04G0329000ZS* exhibited identical expression patterns in various tissues or under stress treatment, suggesting that they may possess analogous functions and exhibit redundancy.

Under varying conditions, *BSK* gene expression profiles were systematically characterized in the current research using transcriptome sequencing data from the BnIR database, providing preliminary evidence for a deeper understanding of the response of *B. napus* to abiotic stress and hormone treatment. This indicated that many *BSK* genes exhibited increased expression under abiotic stress conditions, particularly drought and cold stress (Fig. 10). Although most *BSK* genes exhibited down-regulation after certain hormone treatments, a small subset showed up-regulation in response to hormones (ABA, JA and BL) (Fig. 9). This information provides preliminary evidence that the *BSK* family may be broadly involved in various stress responses throughout plant growth and development. In *Arabidopsis*, *bsk5* mutants show enhanced sensitivity to abscisic acid (ABA) hormones and salt stress (Li *et al.*, 2019; Liu *et al.*, 2022a), while the *bsk134678* mutant seedlings demonstrate enhanced heat resistance compared with wild type. Research has demonstrated that under treatments of heat, cold, external brassinosteroids (BL) and abscisic acid (ABA), many *SoBSKs* in both the heat-sensitive spinach variety Sp73 and the heat-tolerant Sp75 of spinach (*Spinacia oleracea L.*) are differentially regulated (Li *et al.*, 2022), indicating that *SoBSKs* actively participate in plant adaptation mechanisms to temperature fluctuations and hormonal signaling pathways involving BR and ABA. Therefore, homologous clusters in *B. napus* may have similar functions. In this study, 4 *BnaBSK5* genes (*BnaA02G0107400ZS*, *BnaC02G0131400ZS*, *BnaA10G0146000ZS*, and *BnaC09G0424500ZS*) clustered with the *Arabidopsis BSK5* subfamily, showing a similar pattern of response under ABA treatment, indicating their involvement in the abscisic acid pathway (Zhang *et al.*, 2024). The observation aligns with the presence of ABA-responsive elements in their promoter regions. The expression of *BSKs* in cotton increased significantly with salt induction (Lei *et al.*, 2023), and the overexpression of *ZmBSK1* and *ZmBSK7* enhanced salt tolerance in maize (*Zea mays L.*) (Liu *et al.*, 2022a; Zhang *et al.*, 2024). BnaBSK1 expression increased at 6 h of ABA treatment and at 12 h of salt treatment (*BnaA01G0031400ZS*, *BnaC01G0036400ZS*, *BnaA08G0130400ZS*, and *BnaC03G0738400ZS*), suggesting that BnaBSK1 likely participates in rapeseed modulation of salinity adaptation. Further experiments will be conducted to verify these functions.

Under drought and salt stress conditions, different *BnaBSK* genes exhibited distinct expression patterns (Fig. 11). Under PEG treatment, *BnaA01G0031400ZS* and *BnaC01G0036400ZS* showed rapid and significant upregulation as early as 3 hours, indicating their immediate responsiveness to osmotic stress. *BnaC07G0249700ZS* and *BnaA06G0423600ZS* exhibited downregulation during the same timeframe, suggesting they may possess negative regulatory functions or stress evasion mechanisms. The expression trends of *BnaC07G0249700ZS* and *BnaA06G0423600ZS* under drought conditions aligned with transcriptomic data, validating the reliability of transcriptomic-based preliminary screening for identifying stress-responsive *BnaBSK* genes. *BnaA09G0149600ZS* and *BnaC09G0162900ZS* (selected based on their drought-responsive *cis*-elements) did not show early responses but were significantly induced after 12 hours of salt stress, potentially highlighting their specific roles in ion stress adaptation rather than osmotic stress adaptation. Differential expression patterns between PEG and NaCl treatments suggest that *BnaBSK* genes may participate in distinct signaling pathways triggered by different stress stimuli. For example, *BnaA01G0031400ZS* and

*BnaC01G0036400ZS* were strongly upregulated under drought stress but not under salt stress, suggesting functional specificity in osmoregulation or ABA-mediated signaling, consistent with previous reports of *BSK* regulating ABA sensitivity and drought responses in *Arabidopsis* (Li *et al.*, 2021; Ando *et al.*, 2024). The salt-induced upregulation of *BnaA09G0149600ZS* and *BnaC09G0162900ZS* aligned with findings in maize, where *BSK* homologs enhanced salt tolerance through ROS homeostasis and ion transport regulation (Zhu *et al.*, 2016; Liu *et al.*, 2021; Liu *et al.*, 2022b; Zhang *et al.*, 2024). Differences in expression between homologous gene pairs (such as *BnaA01G0031400ZS*/*BnaC01G0036400ZS* and *BnaA09G0149600ZS*/*BnaC09G0162900ZS*) further reflect subfunctionalization or novel functionalization following polyploidization, a common evolutionary trajectory in *Brassica* species. This functional diversification likely enables *B. napus* to finely regulate stress responses across different tissues and developmental stages. These findings indicate that the *BnaBSK* gene is a component of the stress response network in *B. napus*, with individual members playing specialized roles in drought or salt adaptation. These findings not only deepen our understanding of BR-mediated stress signaling mechanisms but also identify candidate genes for future genetic engineering efforts aimed at enhancing rapeseed tolerance to abiotic stresses.

Expression profiling analysis indicates that *BnaA01G0031400ZS* and *BnaC01G0036400ZS* maintain consistently high expression levels under multiple tissues and stress conditions, suggesting their potential role as core signaling components in fundamental regulatory networks. Natural variation in these two genes may correlate with stress tolerance diversity in *B. napus* germplasm resources. Future candidate gene association studies could explore their linkage to stress-tolerance traits. *BnaA01G0031 400ZS* and *BnaC01G0036400ZS* showed rapid and significant upregulation under PEG-simulated drought conditions; *BnaA09G0149600ZS* and *BnaC09G01629 00ZS* exhibited specific induction to salt stress. This differentiated response pattern provides a strategy for gene aggregation breeding: through hybridization and molecular marker-assisted selection, drought-tolerant alleles and salt-tolerant alleles can be polymerized into the same elite variety to achieve yield stability improvement under multiple stress conditions. The promoter regions of these genes are rich in a variety of stress response elements. Linking these stress-inducible promoters with other stress-responsive effector genes enables precise regulation in transgenic or gene-edited crops. The aforementioned genes are promising candidates for improving *B. napus* stress resistance. They enable transgenic approaches or marker-assisted breeding to pyramid superior alleles, offering broad practical potential.

## Conclusions

The study characterizes the *BSK* gene family across the *Brassica napus* genome, highlighting their evolutionary dynamics, structural diversity, and functional versatility. These findings have significant implications for genetic improvement programs aimed at enhancing crop performance, stress tolerance, and yield. Elucidating *BSK* regulatory mechanisms will enable targeted genetic manipulation strategies for harnessing the potential of *B. napus* as a global oilseed crop.

**Author's Contributions: KMZ:** analyzed the data, wrote the manuscript. **WDZ:** analyzed the data, wrote the manuscript. **RS:** analyzed the data. **QFM:** analyzed the data. **HFG:** analyzed the data. **ZCJ:** analyzed the data. **XLT:** Review the manuscript. All authors read and approved the final version.

**Declaration of Competing Interest:** The authors declare that they have no known competing financial interests or personal relationships that could have appeared to influence the work reported in this paper.

**Funding:** This work was supported by the National Key Research and Development Program of China (2024YFD1200400 and 2023YFF1000701), the National Natural Science Foundation of China (32472106), and Jiangsu Provincial Key Research and Development Program (Modern Agriculture) (BE2023342).

### References

Ando, E., K. Taki, T. Suzuki and T. Kinoshita. 2024. A novel semi-dominant mutation in *brassinosteroid signaling kinase1* increases stomatal density. *Front. Plant Sci.*, 15: 1377352.

Anwar, A., Y. Liu, R. Dong, L. Bai, X. Yu and Y. Li. 2018. The physiological and molecular mechanism of brassinosteroid in response to stress: A review. *Biol. Res.*, 51(1): 46.

Bai, M.Y., J.X. Shang, E. Oh, M. Fan, Y. Bai, R. Zentella, T.P. Sun and Z.Y. Wang. 2012. Brassinosteroid, gibberellin and phytochrome impinge on a common transcription module in Arabidopsis. *Nature Cell Biol.*, 14(8): 810-817.

Chalhoub, B., F. Denoeud, S. Liu, I.A. Parkin, H. Tang, X. Wang, J. Chiquet, H. Belcram, C. Tong, B. Samans, M. Corréa, C. Da Silva, J. Just, C. Falentin, C.S. Koh, I. Le Clainche, M. Bernard, P. Bento, B. Noel, K. Labadie, A. Alberti, M. Charles, D. Arnaud, H. Guo, C. Daviaud, S. Alamery, K. Jabbari, M. Zhao, P.P. Edger, H. Chelaifa, D. Tack, G. Lassalle, I. Mestiri, N. Schnel, M.C. Le Paslier, G. Fan, V. Renault, P.E. Bayer, A.A. Golicz, S. Manoli, T.H. Lee, V.H. Thi, S. Chalabi, Q. Hu, C. Fan, R. Tollenaere, Y. Lu, C. Battail, J. Shen, C.H. Sidebottom, X. Wang, A. Canaguier, A. Chauveau, A. Bérard, G. Deniot, M. Guan, Z. Liu, F. Sun, Y.P. Lim, E. Lyons, C.D. Town, I. Bancroft, X. Wang, J. Meng, J. Ma, J.C. Pires, G.J. King, D. Brunel, R. Delourme, M. Renard, J.M. Aury, K.L. Adams, J. Batley, R.J. Snowdon, J. Tost, D. Edwards, Y. Zhou, W. Hua, A.G. Sharpe, A.H. Paterson, C. Guan and P. Wincker. 2014. Plant genetics. Early allopolyploid evolution in the post-Neolithic *Brassica napus* oilseed genome. *Science*, 345(6199): 950-953.

Chen, B., X. Wang, H. Yu, N. Dong, J. Li, X. Chang, J. Wang, C. Jiang, J. Liu, X. Chi, L. Zha and S. Gui. 2024. Genome-wide analysis of UDP-glycosyltransferases family and identification of UGT genes involved in drought stress of *Platycodon grandiflorus*. *Front. Plant Sci.*, 15: 1363251.

Chen, C., H. Chen, Y. Zhang, H.R. Thomas, M.H. Frank, Y. He and R. Xia. 2020. Tbtools: An integrative toolkit developed for interactive analyses of big biological data. *Mol. Plant*, 13(8): 1194-1202.

Chen, C., Y. Wu, J. Li, X. Wang, Z. Zeng, J. Xu, Y. Liu, J. Feng, H. Chen, Y. He and R. Xia. 2023. Tbtools-ii: A "one for all, all for one" bioinformatics platform for biological big-data mining. *Mol. Plant*, 16(11): 1733-1742.

Chen, Y.Y., H.Q. Lu, K.X. Jiang, Y.R. Wang, Y.P. Wang and J.J. Jiang. 2022. The flavonoid biosynthesis and regulation in *Brassica napus*: A review. *Int. J. Mol. Sci.*, 24(1): 357.

Cheng, F., S. Liu, J. Wu, L. Fang, S. Sun, B. Liu, P. Li, W. Hua and X. Wang. 2011. BRAD, the genetics and genomics database for Brassica plants. *BMC Plant Biol.*, 11: 136.

Choi, S.C., A. Hobolth, D.M. Robinson, H. Kishino and J.L. Thorne. 2007. Quantifying the impact of protein tertiary structure on molecular evolution. *Mol. Biol. Evol.*, 24(8): 1769-1782.

Clouse, S.D. 2011. Brassinosteroids. *Arabidopsis Book*, 9: e0151.

Deng, W., Y. Wang, Z. Liu, H. Cheng and Y. Xue. 2014. Hemi: A toolkit for illustrating heatmaps. *PLoS One*, 9(11): e111988.

Edgar, R.C. 2022. Muscle5: High-accuracy alignment ensembles enable unbiased assessments of sequence homology and phylogeny. *Nature Comm.*, 13(1): 6968.

Fàbregas, N. and A.I. Caño-Delgado. 2014. Turning on the microscope turret: A new view for the study of brassinosteroid signaling in plant development. *Physiol. Plant.*, 151(2): 172-183.

Gao, C., Y. Zhao, W. Wang, B. Zhang, X. Huang, Y. Wang and D. Tang. 2024. BRASSINOSTEROID-SIGNALING KINASE 1 modulates OPEN STOMATA 1 phosphorylation and contributes to stomatal closure and plant immunity. *The Plant J.*, 120(1): 45-59.

Gasteiger, E., A. Gattiker, C. Hoogland, I. Ivanyi, R.D. Appel and A. Bairoch. 2003. Expasy: The proteomics server for in-depth protein knowledge and analysis. *Nucl. Acids Res.*, 31(13): 3784-3788.

Han, C., L. Wang, J. Lyu, W. Shi, L. Yao, M. Fan and M.Y. Bai. 2023. Brassinosteroid signaling and molecular crosstalk with nutrients in plants. *J. Gen. Genom.*, 50(8): 541-553.

Huang, S., Y. Ma, Y. Xu, P. Lu, J. Yang, Y. Xie, J. Gan and L. Li. 2023. Shade-induced RTFL/DVL peptides negatively regulate the shade response by directly interacting with BSKs in Arabidopsis. *Nature Comm.*, 14(1): 6898.

Jia, Z., R.F.H. Giehl, R.C. Meyer, T. Altmann and N. von Wirén. 2019. Natural variation of *bsk3* tunes brassinosteroid signaling to regulate root foraging under low nitrogen. *Nature Comm.*, 10(1): 2378.

Khan, T.A., S. Kappachery, S. Karumannil, M. AlHosani, N. Almansoori, H. Almansoori, M. Yusuf, L.P. Tran and M.A. Gururani. 2023. Brassinosteroid signaling pathways: Insights into plant responses under abiotic stress. *Int. J. Mol. Sci.*, 24(24): 17246.

Kim, T.W., S. Guan, Y. Sun, Z. Deng, W. Tang, J.X. Shang, Y. Sun, A.L. Burlingame and Z.Y. Wang. 2009. Brassinosteroid signal transduction from cell-surface receptor kinases to nuclear transcription factors. *Nature Cell Biol.*, 11(10): 1254-1260.

Koch, M.A., B. Haubold and T. Mitchell-Olds. 2000. Comparative evolutionary analysis of chalcone synthase and alcohol dehydrogenase loci in Arabidopsis, Arabis, and related genera (Brassicaceae). *Mol. Biol. Evol.*, 17(10): 1483-1498.

Lamesch, P., T.Z. Berardini, D. Li, D. Swarbreck, C. Wilks, R. Sasidharan, R. Muller, K. Dreher, D.L. Alexander, M. Garcia-Hernandez, A.S. Karthikeyan, C.H. Lee, W.D. Nelson, L. Ploetz, S. Singh, A. Wensel and E. Huala. 2012. The Arabidopsis Information Resource (TAIR): improved gene annotation and new tools. *Nucl. Acids Res.*, 40(Database issue): D1202-1210.

Lei, Y., Y. Cui, R. Cui, X. Chen, J. Wang, X. Lu, D. Wang, S. Wang, L. Guo, Y. Zhang, C. Rui, Y. Fan, M. Han, L. Zhao, H. Zhang, X. Liu, N. Xu, J. Wang, H. Huang, X. Feng, Y. Xi, K. Ni, M. Zhang, T. Jiang and W. Ye. 2023. Characterization and gene expression patterns analysis implies BSK family genes respond to salinity stress in cotton. *Front. Gen.*, 14: 1169104.

Lescot, M., P. Déhais, G. Thijs, K. Marchal, Y. Moreau, Y. Van de Peer, P. Rouzé and S. Rombauts. 2002. Plantcare, a database of plant cis-acting regulatory elements and a portal to tools for in silico analysis of promoter sequences. *Nucl. Acids Res.*, 30(1): 325-327.

Letunic, I. and P. Bork. 2024. Interactive Tree of Life (iTOL) v6: recent updates to the phylogenetic tree display and annotation tool. *Nucl. Acids Res.*, 52(W1): W78-82.

Letunic, I., S. Khedkar and P. Bork. 2021. Smart: Recent updates, new developments and status in 2020. *Nucl. Acids Res.*, 49(D1): D458-460.

Li, Q., F. Xu, Z. Chen, Z. Teng, K. Sun, X. Li, J. Yu, G. Zhang, Y. Liang, X. Huang, L. Du, Y. Qian, Y. Wang, C. Chu and J. Tang. 2021. Synergistic interplay of ABA and BR signal in regulating plant growth and adaptation. *Nature Plants*, 7(8): 1108-1118.

Li, Y., H. Zhang, Y. Zhang, Y. Liu, Y. Li, H. Tian, S. Guo, M. Sun, Z. Qin and S. Dai. 2022. Genome-wide identification and expression analysis reveals spinach brassinosteroid-signaling kinase (BSK) gene family functions in temperature stress response. *BMC Genom.*, 23(1): 453.

Li, Z., J. Shen and J. Liang. 2019. Genome-wide identification, expression profile, and alternative splicing analysis of the brassinosteroid-signaling kinase (BSK) family genes in Arabidopsis. *Int. J. Mol. Sci.*, 20(5): 1138.

Li, Z.Y., Z.S. Xu, G.Y. He, G.X. Yang, M. Chen, L.C. Li and Y.Z. Ma. 2012. A mutation in Arabidopsis BSK5 encoding a brassinosteroid-signaling kinase protein affects responses to salinity and abscisic acid. *Biochem. Biophy. Res. Comm.*, 426(4): 522-527.

Liu, D., L. Yu, L. Wei, P. Yu, J. Wang, H. Zhao, Y. Zhang, S. Zhang, Z. Yang, G. Chen, X. Yao, Y. Yang, Y. Zhou, X. Wang, S. Lu, C. Dai, Q.Y. Yang and L. Guo. 2021. BnTIR: an online transcriptome platform for exploring RNA-seq libraries for oil crop *Brassica napus*. *Plant Biotech. J.*, 19(10): 1895-1897.

Liu, F., P.Y. Qu, J.P. Li, L.N. Yang, Y.J. Geng, J.Y. Lu, Y. Zhang and S. Li. 2024. Arabidopsis protein *S*-acyl transferases positively mediate BR signaling through S-acylation of BSK1. *Proceedings of the National Academy of Sciences of the United States of America*, 121(7): e2322375121.

Liu, L., Y. Sun, P. Di, Y. Cui, Q. Meng, X. Wu, Y. Chen and J. Yuan. 2022a. Overexpression of a *Zea mays* Brassinosteroid-Signaling Kinase gene *ZmBSK1* confers salt stress tolerance in maize. *Front. Plant Sci.*, 13: 894710.

Liu, L., Y. Sun, M. Zhang, R. Liu, X. Wu, Y. Chen and J. Yuan. 2022b. $ZmBSK_1$ positively regulates BR-induced $H_2O_2$ production via NADPH oxidase and functions in oxidative stress tolerance in maize. *Plant Physiol. Biochem.*, 185: 325-335.

Liu, L., Y. Xiang, J. Yan, P. Di, J. Li, X. Sun, G. Han, L. Ni, M. Jiang, J. Yuan and A. Zhang. 2021. BRASSINOSTEROID-SIGNALING KINASE 1 phosphorylating CALCIUM/ CALMODULIN-DEPENDENT PROTEIN KINASE functions in drought tolerance in maize. *New Phytol.*, 231(2): 695-712.

Minh, B.Q., H.A. Schmidt, O. Chernomor, D. Schrempf, M.D. Woodhams, A. von Haeseler and R. Lanfear. 2020. IQ-TREE 2: New models and efficient methods for phylogenetic inference in the genomic era. *Mol. Biol. Evol.*, 37(5): 1530-1534.

Mistry, J., S. Chuguransky, L. Williams, M. Qureshi, G.A. Salazar, E.L.L. Sonnhammer, S.C.E. Tosatto, L. Paladin, S. Raj, L.J. Richardson, R.D. Finn and A. Bateman. 2021. Pfam: The protein families database in 2021. *Nucl. Acids Res.*, 49(D1): D412-d419.

Neu, A., E. Eilbert, L.Y. Asseck, D. Slane, A. Henschen, K. Wang, P. Bürgel, M. Hildebrandt, T.J. Musielak, M. Kolb, W. Lukowitz, C. Grefen and M. Bayer. 2019. Constitutive signaling activity of a receptor-associated protein links fertilization with embryonic patterning in *Arabidopsis thaliana*. *Proceedings of the National Academy of Sciences of the United States of America*, 116(12): 5795-5804.

Nolan, T.M., N. Vukašinović, D. Liu, E. Russinova and Y. Yin. 2020. Brassinosteroids: Multidimensional regulators of plant growth, development, and stress responses. *Plant Cell*, 32(2): 295-318.

Peres, A., J.S. Soares, R.G. Tavares, G. Righetto, M.A.T. Zullo, N.B. Mandava and M. Menossi. 2019. Brassinosteroids, the sixth class of phytohormones: A molecular view from the discovery to hormonal interactions in plant development and stress adaptation. *Int. J. Mol. Sci.*, 20(2): 331.

Qanmber, G., Z. Liu, F. Li and Z. Yang. 2024. Brassinosteroids in cotton: Orchestrating fiber development. *New Phytol.*, 244(5): 1732-1741.

Ren, H., B.C. Willige, Y. Jaillais, S. Geng, M.Y. Park, W.M. Gray and J. Chory. 2019. BRASSINOSTEROID-SIGNALING KINASE 3, a plasma membrane-associated scaffold protein involved in early brassinosteroid signaling. *PLoS Gen.*, 15(1): e1007904.

Ren, R., X. Yang, J. Xu, K. Zhang, M. Zhang, G. Liu, X. Yao, L. Lou, J. Xu, L. Zhu and Q. Hou. 2021. Genome-wide identification and analysis of promising GDSL-type lipases related to gummy stem blight resistance in watermelon (*Citrullus lanatus*). *Scientia Horticulturae*, 289: 110461.

Sarwar, R., T. Jiang, P. Ding, Y. Gao, X. Tan and K. Zhu. 2021. Genome-wide analysis and functional characterization of the DELLA gene family associated with stress tolerance in *B. napus*. *BMC Plant Biol.*, 21(1): 286.

Shi, B., Y. Wang, L. Wang and S. Zhu. 2024. Genome-wide identification of the brassinosteroid signal kinase gene family and its profiling under salinity stress. *Int. J. Mol. Sci.*, 25(15): 8499.

Shi, H., Q. Li, M. Luo, H. Yan, B. Xie, X. Li, G. Zhong, D. Chen and D. Tang. 2022. BRASSINOSTEROID-SIGNALING KINASE1 modulates MAP KINASE15 phosphorylation to confer powdery mildew resistance in Arabidopsis. *Plant Cell*, 34(5): 1768-1783.

Shiu, S.H., W.M. Karlowski, R. Pan, Y.H. Tzeng, K.F. Mayer and W.H. Li. 2004. Comparative analysis of the receptor-like kinase family in Arabidopsis and rice. *Plant Cell*, 16(5): 1220-1234.

Słomnicka, R., M. Cieplak, A.M. Martín-Hernández and G. Bartoszewski. 2025. Brassinosteroids in cucurbits: Modulators of plant growth architecture and stress response. *Int. J. Mol. Sci.*, 26(15): 7234.

Sreeramulu, S., Y. Mostizky, S. Sunitha, E. Shani, H. Nahum, D. Salomon, L.B. Hayun, C. Gruetter, D. Rauh, N. Ori and G. Sessa. 2013. BSKs are partially redundant positive regulators of brassinosteroid signaling in Arabidopsis. *The Plant J.*, 74(6): 905-919.

Su, B., X. Zhang, L. Li, S. Abbas, M. Yu, Y. Cui, F. Baluška, I. Hwang, X. Shan and J. Lin. 2021. Dynamic spatial reorganization of BSK1 complexes in the plasma membrane underpins signal-specific activation for growth and immunity. *Mol. Plant*, 14(4): 588-603.

Swift, M.L. 1997. Graphpad prism, data analysis, and scientific graphing. *J. Chem. Inform. Comp. Sci.*, 37(2): 411-412.

Tang, W., T.W. Kim, J.A. Oses-Prieto, Y. Sun, Z. Deng, S. Zhu, R. Wang, A.L. Burlingame and Z.Y. Wang. 2008. BSKs mediate signal transduction from the receptor kinase BRI1 in Arabidopsis. *Science*, 321(5888): 557-560.

Tian, P., J. Liu, B. Yan, C. Zhou, H. Wang and R. Shen. 2023. BRASSINOSTEROID-SIGNALING KINASE1-1, a positive regulator of brassinosteroid signalling, modulates plant architecture and grain size in rice. *J. Exp. Bot.*, 74(1): 283-295.

Vukašinović, N., T.M. Nolan and E. Russinova. 2025. Unlocking the potential of brassinosteroids: A path to precision plant engineering. *Science*, 390(6773): eadu9798.

Wang, J., L. Liu, R. Luo, Q. Zhang, X. Wang, F. Ling and P. Wang. 2024. Genome-wide analysis of filamentous temperature-sensitive H protease (ftsH) gene family in soybean. *BMC Genom.*, 25(1): 524.

Wang, J., H. Shi, L. Zhou, C. Peng, D. Liu, X. Zhou, W. Wu, J. Yin, H. Qin, W. Ma, M. He, W. Li, J. Wang, S. Li and X. Chen. 2017. OsBSK1-2, an orthologous of AtBSK1, is involved in rice immunity. *Front. Plant Sci.*, 8: 908.

Wang, L., X. Yin, C. Cheng, H. Wang, R. Guo, X. Xu, J. Zhao, Y. Zheng and X. Wang. 2015. Evolutionary and expression analysis of a MADS-box gene superfamily involved in ovule development of seeded and seedless grapevines. *Mol. Gen. Genom.*, 290(3): 825-846.

Wang, L., Z. Zhao, H. Li, D. Pei, Z. Huang, H. Wang and L. Xiao. 2024. Genome-wide identification of *NDPK* family genes and expression analysis under abiotic stress in *Brassica napus*. *Int. J. Mol. Sci.*, 25(12): 6795.

Wang, X., Z. Diao, C. Cao, Y. Liu, N. Xia, Y. Zhang, L. Lu, F. Kong, H. Zhou, L. Chen, J. Zhang, B. Wang, R. Huang, D. Tang and S. Li. 2024. The receptor-like cytoplasmic kinase OsBSK1-2 regulates immunity via an HLH/bHLH complex. *J. Integ. Plant Biol.*, 66(12): 2754-2771.

Wang, Z., B.X. Wang, F.Y. Zhao and J. Cao. 2020. Genome-wide analysis of chitinase gene family in rice and *Arabidopsis* reveal their mechanisms and diverse roles in defense response. *Int. J. Agri. Biol.*, 24(4): 812-822.

Wang, Z.Y., M.Y. Bai, E. Oh and J.Y. Zhu. 2012. Brassinosteroid signaling network and regulation of photomorphogenesis. *Ann. Rev. Gen.*, 46: 701-724.

Wang, Z.Y., H. Seto, S. Fujioka, S. Yoshida and J. Chory. 2001. BRI1 is a critical component of a plasma-membrane receptor for plant steroids. *Nature*, 410(6826): 380-383.

Wu, X., F. Chen, X. Zhao, C. Pang, R. Shi, C. Liu, C. Sun, W. Zhang, X. Wang and J. Zhang. 2021. QTL mapping and GWAS reveal the genetic mechanism controlling soluble solids content in *Brassica napus* shoots. *Foods*, 10(10): 2400.

Xia, X., H. Dong, Y. Yin, X. Song, X. Gu, K. Sang, J. Zhou, K. Shi, Y. Zhou, C.H. Foyer and J. Yu. 2021. Brassinosteroid signaling integrates multiple pathways to release apical dominance in tomato. *Proceedings of the National Academy of Sciences of the United States of America*, 118(11): e2004384118.

Yan, H., Y. Zhao, H. Shi, J. Li, Y. Wang and D. Tang. 2018. BRASSINOSTEROID-SIGNALING KINASE1 phosphorylates MAPKKK5 to regulate immunity in Arabidopsis. *Plant Physiol.*, 176(4): 2991-3002.

Yan, P., Y. Wang, J. Cui, M. Liu, Y. Zhu, F. Ma, Y. Liu, D. Lan, S. Dong, Z. Hu, F. Niu, Y. Liu, X. Zhang, S. He, J. Hu, X. Yuan, Y. Li, J. Yang, L. Cao and X. Luo. 2025. OsMAPKKK5 affects brassinosteroid signal transduction via phosphorylating OsBSK1-1 and regulates rice plant architecture and yield. *Plant Biotech. J.*, 23(5): 1798-1813.

Yang, Z., S. Wang, L. Wei, Y. Huang, D. Liu, Y. Jia, C. Luo, Y. Lin, C. Liang, Y. Hu, C. Dai, L. Guo, Y. Zhou and Q.Y. Yang. 2023. BnIR: A multi-omics database with various tools for *Brassica napus* research and breeding. *Mol. Plant*, 16(4): 775-789.

Ye, Z., F. Hu, W. Zhang, D. Fang, K. Dong and J. Cao. 2023. Amino acid transporters of *Brassica napus*: Identification, evolution, expression and response to various stresses. *Ind. Crops Prod.*, 194: 116338.

Zeytuni, N. and R. Zarivach. 2012. Structural and functional discussion of the tetra-trico-peptide repeat, a protein interaction module. *Structure*, 20(3): 397-405.

Zhang, B., X. Wang, Z. Zhao, R. Wang, X. Huang, Y. Zhu, L. Yuan, Y. Wang, X. Xu, A.L. Burlingame, Y. Gao, Y. Sun and W. Tang. 2016. OsBRI1 activates BR signaling by preventing binding between the TPR and kinase domains of OsBSK3 via phosphorylation. *Plant Physiol.*, 170(2): 1149-1161.

Zhang, C., Y. Miao, Y. Xiang and A. Zhang. 2024. Brassinosteroid-signaling kinase ZmBSK7 enhances salt stress tolerance in maize. *Biochem. Biophys. Res. Comm.*, 723: 150222.

Zhang, L., W. Sun, W. Gao, Y. Zhang, P. Zhang, Y. Liu, T. Chen and D. Yang. 2024. Genome-wide identification and analysis of the GGCT gene family in wheat. *BMC Genom.*, 25(1): 32.

Zhang, S., X. Hu, J. Dong, M. Du, J. Song, S. Xu and C. Zhao. 2022. Identification, evolution, and expression analysis of OsBSK gene family in Oryza sativa Japonica. *BMC Plant Biol.*, 22(1): 565.

Zhao, T., X. Cao, S. Eroğlu, Y. Xia, A. ElGamal, H.S. Abdelkader, J. Liu and Y. Wang. 2025. BRASSINOSTEROID-SIGNALING KINASEs: Small family, big functions. *Physiologia Plantarum*, 177(5): e70555.

Zhao, Y., G. Wu, H. Shi and D. Tang. 2019. RECEPTOR-LIKE KINASE 902 associates with and phosphorylates BRASSINOSTEROID-SIGNALING KINASE1 to regulate plant immunity. *Mol. Plant*, 12(1): 59-70.

Zhu, Y., J. Yan, W. Liu, L. Liu, Y. Sheng, Y. Sun, Y. Li, H.V. Scheller, M. Jiang, X. Hou, L. Ni and A. Zhang. 2016. Phosphorylation of a NAC transcription factor by a Calcium/Calmodulin-dependent protein kinase regulates abscisic acid-induced antioxidant defense in maize. *Plant Physiol.*, 171(3): 1651-1664.

Zolkiewicz, K. and D. Gruszka. 2024. Take a deep breath: Manipulating brassinosteroid homeostasis helps cereals adapt to environmental stress. *Plant Physiol.*, 197(1): kiaf003.